

## Surface exchange of nitric oxide, nitrogen dioxide, and ozone at a cattle pasture in Rondônia, Brazil

G. A. Kirkman,<sup>1</sup> A. Gut,<sup>1</sup> C. Ammann,<sup>1</sup> L. V. Gatti,<sup>2</sup> A. M. Cordova,<sup>2</sup> M. A. L. Moura,<sup>3</sup> M. O. Andreae,<sup>1</sup> and F. X. Meixner<sup>1</sup>

Received 21 February 2001; revised 4 December 2001; accepted 17 December 2001; published 10 October 2002.

[1] Measurements of NO–NO<sub>2</sub>–O<sub>3</sub> trace gas exchange were performed for two transition season periods during the La Niña year 1999 (30 April to 17 May, “wet–dry,” and 24 September to 27 October, “dry–wet”) over a cattle pasture in Rondônia. A dynamic chamber system (applied during the dry–wet season) was used to directly measure emission fluxes of nitric oxide (NO) and surface resistances for nitrogen dioxide (NO<sub>2</sub>) and ozone (O<sub>3</sub>) deposition. A companion study was simultaneously performed in an old-growth forest. In order to determine ecosystem-representative NO<sub>2</sub> and O<sub>3</sub> deposition fluxes for both measurement periods, an inferential method (multiresistance model) was applied to measure ambient NO<sub>2</sub> and O<sub>3</sub> concentrations using observed quantities of turbulent transport. Supplementary measurements included soil NO diffusivity and soil nutrient analysis. The observed NO soil emission fluxes were nine times lower than old-growth rain forest emissions under similar soil moisture and temperature conditions and were attributed to the combination of a reduced soil N cycle and lower effective soil NO diffusion at the pasture. Canopy resistances ( $R_c$ ) of both gases controlled the deposition processes during the day for both measurement periods. Day and night NO<sub>2</sub> canopy resistances were significantly similar ( $\alpha = 0.05$ ) during the dry–wet period. Ozone canopy resistances revealed significantly higher daytime resistances of 106 s m<sup>-1</sup> versus 65 s m<sup>-1</sup> at night because of plant, soil, and wet skin uptake processes, enhanced by stomatal activity at night and aqueous phase chemistry on vegetative and soil surfaces. The surface of the pasture was a net NO<sub>x</sub> sink during 1999, removing seven times more NO<sub>2</sub> from the atmosphere than was emitted as NO. **INDEX TERMS:** 0315 Atmospheric Composition and Structure: Biosphere/atmosphere interactions

**Citation:** Kirkman, G. A., A. Gut, C. Ammann, L. V. Gatti, A. M. Cordova, M. A. L. Moura, M. O. Andreae, and F. X. Meixner, Surface exchange of nitric oxide, nitrogen dioxide, and ozone at a cattle pasture in Rondônia, Brazil, *J. Geophys. Res.*, 107(D20), 8083, doi:10.1029/2001JD000523, 2002.

### 1. Introduction

[2] Over the last 25 years, more than 70 million ha of the native vegetation in Brazil have been replaced by pastures mostly planted to grasses of the African genus *Brachiaria* for cattle grazing. Rondônia has seen a large proportion of this development and stands today as one of the best examples of how rapidly South American tropical ecosystems are undergoing anthropogenic change. Several years after deforestation and establishment of agriculture, there is a marked decline in soil productivity and crop yields, forcing farmers to either abandon their land or establish permanent agriculture [Moran, 1993]. Changes in soil

productivity are accompanied by changes in the air–surface exchanges of trace gases such as nitrogen oxides (NO<sub>x</sub> = NO + NO<sub>2</sub>) and ozone (O<sub>3</sub>).

[3] The measurement of all three species of the NO<sub>2</sub>–NO–O<sub>3</sub> triad is necessary for studying and making inferences on the air–surface exchanges at the landscape scale. First, the fast chemical reactions of nitric oxide (NO) with O<sub>3</sub> or peroxy radicals, which form nitrogen dioxide (NO<sub>2</sub>) [Crutzen, 1995; Kolar, 1990], and the reverse photodissociation of NO<sub>2</sub> during the day (<400 nm), occur on time-scales of minutes, the same timescales for turbulence mixing at the surface [Kramm *et al.*, 1991]. Second, the gases are governed by quite different air–surface exchange regulating processes. For instance, the predominant natural source of NO is the soil where biotic (nitrification and denitrification) and abiotic (chemodenitrification) processes produce this gas. Within the soil environment, the aerobic process of nitrification (predominant at <60% water-filled pore space–WFPS) is maintained primarily by autotrophic bacteria resulting in the conversion of ammonium (NH<sub>4</sub><sup>+</sup>) to nitrate (NO<sub>3</sub><sup>-</sup>) via nitrite (NO<sub>2</sub><sup>-</sup>). There are two groups of

<sup>1</sup>Biogeochemistry Department, Max Planck Institute for Chemistry, Mainz, Germany.

<sup>2</sup>Divisão de Química Ambiental, Instituto de Pesquisas Energeticas e Nucleares (IPEN), São Paulo, Brazil.

<sup>3</sup>Departamento de Meteorologia, Centro de Ciencia Exatas e Naturais, Universidade Federal de Alagoas, Maceió Alagoas, Brazil.

nitrifiers, namely the ammonium oxidizing nitrifiers, which convert  $\text{NH}_4^+$  via hydroxylamine to  $\text{NO}_2^-$ , and the nitrite oxidizing nitrifiers, which oxidize  $\text{NO}_2^-$  to  $\text{NO}_3^-$ . Denitrification on the other hand is an anaerobic process (predominant at >60% WFPS) in which denitrifiers reduce  $\text{NO}_3^-$  via  $\text{NO}_2^-$ , NO and nitrous oxide ( $\text{N}_2\text{O}$ ) to molecular nitrogen ( $\text{N}_2$ ). The complete denitrification pathway results in the reduction of  $\text{NO}_3^-$  to  $\text{N}_2$ , but significant amounts of NO and  $\text{N}_2\text{O}$  can be emitted before complete reduction to  $\text{N}_2$  [Remde and Conrad, 1991; Remde et al., 1989; Cardenas et al., 1993]. Soil pH, metallic ion composition, and soil organic matter (SOM) all control the abiotic process of chemodenitrification, whereby microbially produced  $\text{NO}_2^-$  is decomposed to NO and  $\text{NO}_2$  [van Cleemput and Baert, 1984; Davidson, 1992].

[4] Recent work in Rondônia has shown that NO fluxes from old pastures can be 25 times lower than fluxes from adjacent forest [Garcia-Montiel et al., 2002]. Further, Davidson et al. [2000] found for a variety of tropical sites in Costa Rica, Puerto Rico, and Brazil that old tropical pastures produce consistently lower NO fluxes than old-growth tropical forests. The reasons for these differences between the two ecosystems are changes in the environmental factors controlling NO emissions. These factors include a combination of soil water, temperature, nutrient status, pH, diffusion, plant biomass characteristics, and ambient atmospheric conditions [Davidson et al., 2000; Ludwig et al., 2001].

[5] The air–surface exchanges of  $\text{O}_3$  and  $\text{NO}_2$  occur via dry deposition onto vegetation (plant stomata/cuticle), onto bare soil surfaces, or into solution with surface water [Meixner, 1994a]. The rate at which plant stomatal uptake occurs is determined by the concentration gradient between the gas phase inside and outside the leaf, leaf temperature, water vapor deficit, and intensity of photosynthetic radiation, although some uncertainty surrounds the magnitudes of these processes, particularly for  $\text{NO}_2$  [Lerdau et al., 2000]. Removal rates of  $\text{O}_3$  by soils with high levels of organic matter and moderate moisture content have been shown to be significant [Wesely and Hicks, 2000]. Less is known about bare soil as a  $\text{NO}_2$  sink. There are, however, reports of  $\text{NO}_2$  reactions with humic acids and phenols on dry soils and stone surfaces [Baumgartner et al., 1992] and chemical scavenging ( $\text{NO}_2 + \text{NO}_2^- \rightarrow \text{NO}_3^- + \text{NO}$ ) in low pH, high SOM content soils [van Cleemput and Baert, 1976]. Recent work suggests some ammonia oxidizers are able to consume  $\text{NO}_2$  and produce NO and  $\text{NO}_2^-$  under both oxic and anoxic soil conditions [Zart and Bock, 1998; Schmidt and Bock, 1997]. Equally unclear are the effects of wet surface uptake, for which aqueous phase chemistry has been reported to enhance  $\text{O}_3$  deposition to foliage [Fuentes et al., 1992].

[6] As part of the European Studies on Trace Gases and Atmospheric Chemistry within the Large-Scale Biosphere-Atmosphere Experiment in Amazonia project (LBA-EUSTACH), results from measurements over a cattle pasture in Rondônia (cf. section 2.1) are presented. A companion study was simultaneously performed in an old-growth forest (see companion papers by Gut et al. [2002a, 2002b]). Measurements were performed during both the LBA-EUSTACH-1 and LBA-EUSTACH-2 campaigns [Andreae et al., 2002], which represent two transition seasons during 1999 (30 April to 17 May, wet–dry, and 24 September to 27 October, dry–wet), a La Niña year. The objectives of this

study were to (1) quantify the air exchanges of NO,  $\text{NO}_2$ , and  $\text{O}_3$  for an established cattle pasture during two distinct seasons, (2) propose possible reasons for the expected lower NO emission fluxes from the pasture in light of those from an old-growth primary forest for the same period, and (3) examine and discuss the surface resistances and deposition fluxes of  $\text{NO}_2$  and  $\text{O}_3$  and their possible environmental controlling factors.

## 2. Experimental

[7] The primary tool used for gas exchange measurements was a dynamic chamber system (applied during LBA-EUSTACH-2 only), which measured emission and deposition fluxes of NO,  $\text{NO}_2$  and  $\text{O}_3$  (cf. section 2.3). In order to determine ecosystem-representative  $\text{NO}_2$  and  $\text{O}_3$  deposition fluxes for both the LBA-EUSTACH-1 and LBA-EUSTACH-2 periods, an inferential method (multiresistance model) was applied to measured ambient  $\text{NO}_2$  and  $\text{O}_3$  concentrations using observed quantities of turbulent transport (cf. section 2.4). In the case of  $\text{O}_3$ , the resulting fluxes could be compared to a limited data set of independent flux measurements by the aerodynamic gradient approach (cf. section 2.5). Supplementary measurements included soil NO diffusivity and soil nutrient analysis (cf. section 2.6).

### 2.1. Site Description

[8] Rondônia is situated on the fringe of the Amazon basin is comprised of seasonally dry tropical rain forest (*Floresta ombrofila aberta*) and various forms of degraded land (*Floresta de transição*), cultivated land (*plantação*), and pasture (*pastagem*). It is also situated along the “arc of deforestation” of Brazil and is known for its characteristic “fishbone” deforestation pattern and rapid land conversion rates [Andreae et al., 2002]. Human settlement in this area increased considerably after construction in 1968 of the Cuiabá–Porto Velho highway (BR 364), which cut through some of the more fertile parts of the weathered soils in this region [Moran, 1993]. Paving of this highway was completed in 1984. It increased immigration and stimulated markets for agriculture and forest products [Browder and Godfrey, 1997], which led to slash-and-burn agriculture, cropping and established cattle pasture, and abandonment.

[9] The measurement site was located on the commercial cattle ranch *Fazenda Nossa Senhora Aparecida* (FNS) (Figure 1), which lies between the unpaved roads Linha 12 and 16 off the paved RO-470 at 10°45'44"S, 62°21'27"W at an elevation of ca. 315 m. Soils at FNS are highly weathered, sandy (>75%) red-yellow podzols (*Podzólico vermelho amarelo de textura média*-Brasil or *Orthic acrisol*-FAO) [Hodnett et al., 1996]. The nearest town is Ouro Preto d'Oeste, situated on the paved federal highway BR 364 between the towns Jaru and Ji-Paraná, ca. 8 km NE from the site. A small charcoal kiln off the BR 364 ca. 8 km from the site was in operation during the wet–dry season.

[10] The land was first deforested in 1977 by the current owner and planted to rice (*Oryza sativa*, *Agulhinha*/IAC (*comum*)), beans (*Phaseolus vulgaris*, *Carioquinha*, *Rosinha*, *Tibagi*) and maize (*Zea mays*, *Asteca e Híbridos*). Fire was used as the primary deforestation tool and all burns typically took place between June and September. Combustion of slashed material was generally considered to be partial

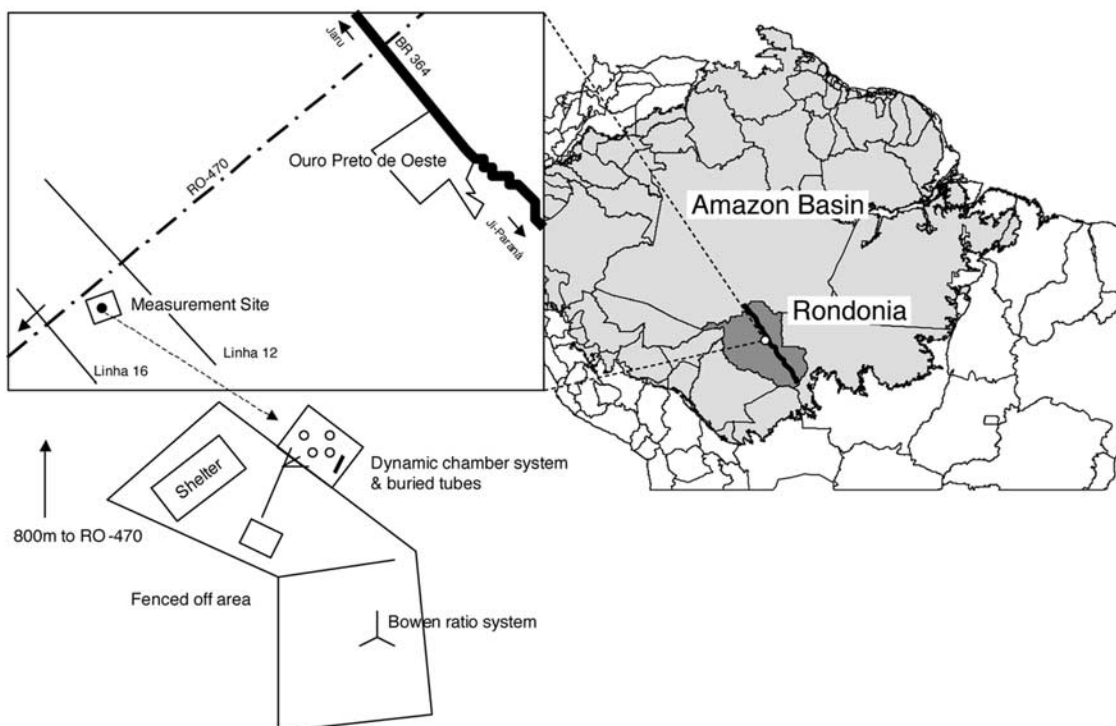


**Figure 1.** Location of the LBA-EUSTACH measurement site *Fazenda Nossa Senhora Aparecida* (FNS) in Rondônia, Brazil.

or poor. The first two seasons of cropping were the most lucrative with yields surpassing those of later years. Thereafter the land underwent a sequence of burn and *Brachiaria decumbens* pasture grass (*Braquiária australiana*, *Braquiária comum*, *Braquiária de alho*, *Capim*) for 12 seasons, after which a disk harrow (20 cm) was used in 1992 to liberate the old-growth forest soil organic matter below the grass root zone. One season of beans was planted, and yields equaled the first two seasons after deforestation. The camp was then burned for two seasons and planted to a predominately homogenous sward of *Brachiaria brizantha* (A. Rich.) Stapf. (*Brachiarão*, *Brizantão*, *Brizantha*, *Braquiario*, *Capim braquiária*, *Capim marandu*, *Capim ocinde*) and thereafter was never burned again. The camp has never been fertilized.

[11] *B. brizantha* is a fire-sensitive exotic perennial grass species with stout erect culms and broadly lanceolate leaf blades, which can reach a height of up to 120 cm if left ungrazed. It produces poor seed and propagates vegetatively [Fernando, 1961]. The sward at FNS had a leaf area index of  $1.2 \text{ m}^2 \text{ m}^{-2}$  (Kirkman, unpublished data, 1990) during the dry-wet season and  $2.1 \text{ m}^2 \text{ m}^{-2}$  during the wet-dry season (Waterloo, personal communication, 2000). Assuming a leaf N content of ca. 0.67%, as found by Davidson (personal communication, 2000) at the *Fazenda Vitoria* in Pará, the total above ground N for FNS was estimated to be  $21 \text{ kg ha}^{-1}$ .

[12] During the measurement campaign FNS was stocked with a breeding herd of *Blanco* cattle (*Bos indicus hybrid*). The grass sward had a carrying capacity of ca. 2 animal units (1 A.U. = 450 kg) per hectare. Soon after deforestation and for a period after the ploughing in 1992, the carrying capacity was in the order of 3–4 A.U.  $\text{ha}^{-1}$ . The 4 cattle pastures at FNS were typically rotated every 3 months, resulting in a camp utilization of 3–4 months per year, depending on sward

conditions. Data from *Fazenda Vitoria* has shown that export of N as cattle harvesting is estimated at about  $7 \text{ kg N ha}^{-1} \text{ yr}^{-1}$ , including return from feces and urine (but excluding  $\text{NH}_3$  volatilization). At the time of measurement the camp was stocked with a breeding herd comprised of cows, heifers and two bulls.

## 2.2. Monitoring of Ambient Trace Gas Concentrations

[13] During the LBA-EUSTACH-1 and LBA-EUSTACH-2 campaigns, concentrations of NO,  $\text{NO}_2$ , and  $\text{O}_3$  were monitored at FNS. A glass tube (2-cm diameter) of a total length of 2.0 m, continuously purged by an auxiliary pump with a flow rate of  $28 \text{ L min}^{-1}$ , was used as the sample intake system. The rain-protected sampling head was mounted 3.5 m above ground on top of an instrument trailer. From a glass manifold mounted inside the trailer, sample air was fed through 1/4 in. PTFE tubing (2 m) to 47 mm PTFE filters ( $0.5 \mu\text{m}$ ) mounted on the sample intake ports of the NO/ $\text{NO}_x$ , and  $\text{O}_3$  analyzers. Commercial gas-phase chemiluminescence and spectrometric analyzers were used to measure NO,  $\text{NO}_2$ , and  $\text{O}_3$  concentrations, respectively (Table 1). NO and  $\text{NO}_2$  calibrations were conducted with the use of a Thermo Environmental Instruments Inc., Model 146C gas phase titration and ozone generator instrument by mixing known concentrations of NO calibration gas with nondried zero air from a Thermo Environmental Instruments Inc., Model 111 zero air supply. To this, a lesser amount of  $\text{O}_3$  was added and the amount of  $\text{NO}_2$  produced was then determined by the measured loss of NO. Subsequently  $\text{O}_3$  was calibrated by assuming that the loss of NO was equivalent to the concentration of  $\text{O}_3$  produced such that

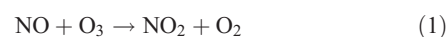


**Table 1.** Trace Gas Detectors, Micrometeorological Instrumentation, and Sensors Used at *Fazenda Nossa Senhora Aparecida* (FNS) during LBA-EUSTACH-2 (24 September to 27 October 1999) and LBA-EUSTACH-1 (30 April to 17 May 1999)

Quantity	Technique or sensor	Model, manufacturer	Detection limit or precision	Integra./excec. or averaging time, s
NO concentration (3.5 m above ground)	Gas-phase chemiluminescence	Model 42C TL (trace level) Thermo Environment Instruments Inc., U.S.A.	0.025 ppb	300
NO <sub>2</sub> concentration (3.5 m above ground)	Catalytic conversion of NO <sub>2</sub> to NO by molybdenum converter (at 300°C) and gas phase chemiluminescence	Model 42C TL (trace level) Thermo Environment Instruments Inc., U.S.A.	0.025 ppb	300
O <sub>3</sub> concentration (3.5 m above ground)	UV absorption, symmetric dual cell design	Model 49C Thermo Environment Instruments Inc., U.S.A.	0.5 ppb	300
NO concentration (dynamic chambers)	Gas-phase chemiluminescence	Model 42C TL (trace level)	0.07 ppb	60/1800
NO <sub>2</sub> concentration (dynamic chambers)	Catalytic conversion of NO <sub>2</sub> to NO by molybdenum converter (at 300°C) and gas phase chemiluminescence	Model 42C TL (trace level) Thermo Environment Instruments Inc., U.S.A.	0.14 ppb	60/1800
O <sub>3</sub> concentration (dynamic chambers)	UV absorption, symmetric dual cell design	Model 49C Thermo Environment Instruments Inc., U.S.A.	0.03 ppb	60/1800
<sup>220</sup> Rn concentration	Alpha particle detection	Alphaguard PQ 2000 Pro, Genitron, Germany	2 Bq m <sup>-3</sup> ± 10%	–
O <sub>3</sub> concentration (aerodynamic gradient)	UV absorption, symmetric dual cell design, switched intakes at 0.53 and 4.5 m above ground	Model 49 Thermo Electron Inc., U.S.A.	0.5 ppb ± 0.56 ppb	2/1800
Soil temperature (dynamic chambers)	Thermistors at 0.05m below ground		–	–
Volumetric soil moisture (dynamic chambers)	Time domain reflectometry (TDL) sensors at 0.05m below ground	TRIME-ES P2M IMKO GmbH, Germany	–	–
Surface wetness (dynamic chambers)	Surface wetness grids at soil surface	237 WSG Campbell Scientific Ltd., U.K.	–	–
Wind speed profile at 0.53, 1.02, 2.02, and 4.50 m above ground	3-cup-anemometers (optical switch)	A100ML Vector Instruments, U.K.	0.25 m/s ± 0.10 m/s	10/1800
Wind direction, 4.50 m above ground	Potentiometric wind vane	W200P Vector Instruments, U.K.	±5°	10/1800
Air temperature profile at 0.53, 1.02, 2.02, and 4.50 m above ground	Fine-wire (0.72µm), nonaspirated thermocouples, chrome-constantan (E-type)	Campbell Scientific Ltd., U.K.	±0.02 K	1/1800
Global radiation flux 2.02 m above ground	Pyranometer sensor	LI200SZ LI-COR Inc., U.S.A.	< ± 3%	10/1800

[14] The NO<sub>x</sub> analyzer employed was equipped with a molybdenum (Mo) NO<sub>2</sub> to NO converter, which is non-specific for determination of NO<sub>2</sub> [Winer *et al.*, 1974; Fehsenfeld *et al.*, 1987]. The instrument also converts other reactive nitrogen compounds to NO, in particular, nitric acid (HNO<sub>3</sub>), nitrous acid (HONO), the nitrate radical (NO<sub>3</sub>), dinitrogen pentoxide (N<sub>2</sub>O<sub>5</sub>), peroxyacetyl nitrate (PAN), and other organic nitrates. PAN is a thermally unstable compound at temperatures well below those found at FNS. HNO<sub>3</sub> was probably the most important of these interfering nitrogenous compounds at FNS. However, HNO<sub>3</sub> is also known for its high affinity to the inner walls of intake systems, especially if these (1) consist of glass and/or stainless steel and (2) are covered with a molecular layer of water, which was certainly the case for the humid conditions at FNS. It is therefore assumed that HNO<sub>3</sub> (and also HNO<sub>2</sub>, if present) was completely destroyed within the glass sample line (described above) and stainless steel fittings inside the instruments. Interference from gaseous ammonia (NH<sub>3</sub>) is most unlikely, since the Mo converter was operated at 300°C and conversion of NH<sub>3</sub> is usually not observed for temperatures below 400°C. The other interfering nitro-

genous compounds mentioned above are assumed to be negligible compared to NO<sub>2</sub>.

### 2.3. Dynamic Chamber System

[15] During the LBA-EUSTACH-2 campaign, a second set of identical NO, NO<sub>x</sub>, and O<sub>3</sub> analyzers (Table 1) was applied to a dynamic chamber system. This system was similar to that described by Gut *et al.* [2002a, 2002b]. Weekly NO and NO<sub>2</sub> calibrations were conducted with the same gas-phase titration and zero air supply system described above.

[16] Chamber measurements were used to (1) quantify surface emission fluxes of NO directly and (2) evaluate surface resistances for NO<sub>2</sub> and O<sub>3</sub> by relating chamber fluxes to chamber concentrations (cf. section 2.4). The system comprised three chambers placed over a previously grazed *B. brizantha* sward and sealed to the surface with TEFLON<sup>®</sup> foil weighted by small sandbags (Figure 2), such that no root destructive frames were necessary. Ambient airflow through the chambers was controlled by small air-entry fans (model D243M-012GK-1, Micronel, Switzerland) producing an average flow rate ( $Q$ ) of ca. 28 L min<sup>-1</sup> such that the average air residence time was ca. 25 s. Air inside the

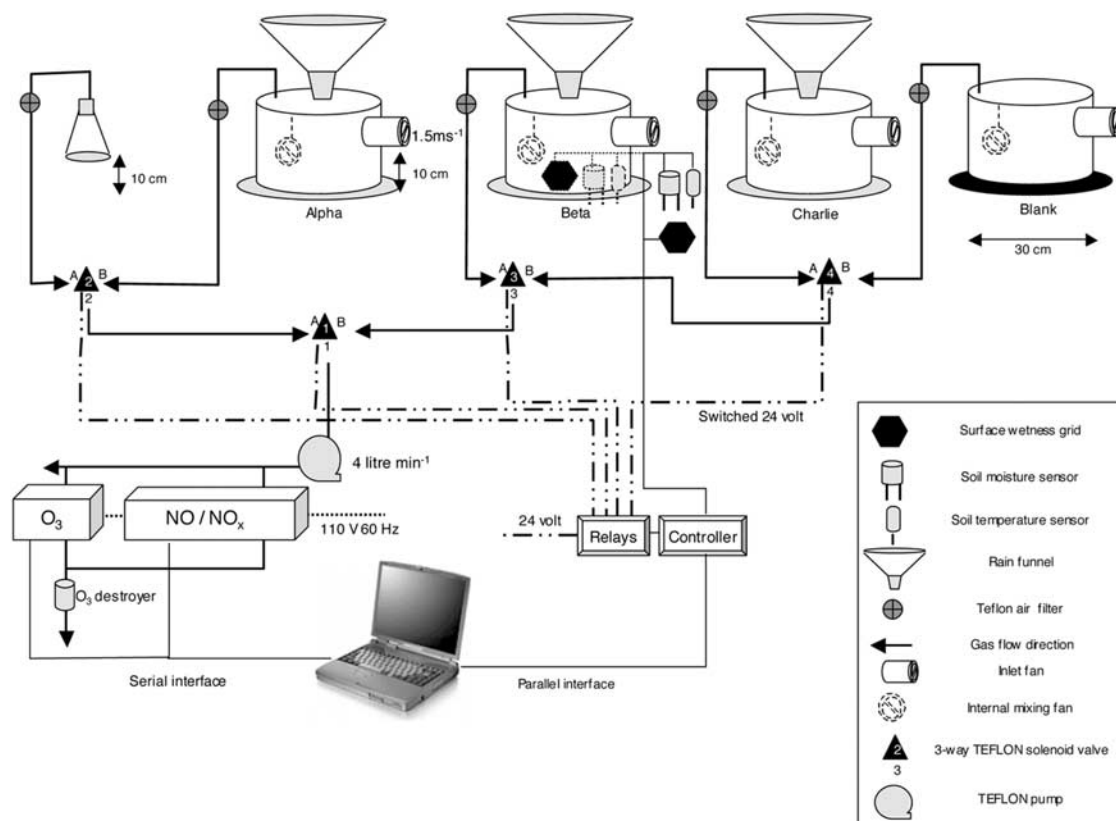


Figure 2. Dynamic chamber system.

chamber was continuously mixed with an additional fan (model F62MM-012GK-0, Micronel, Switzerland) to prevent concentration gradients [Meixner *et al.*, 1997]. A fourth “blank” chamber, closed at the bottom, was employed for in situ quantification of chemical reactions and chamber wall deposition effects (see below). A sample inlet for measurement of ambient NO, NO<sub>2</sub>, and O<sub>3</sub> concentrations was positioned close to the inlet of one of the chambers (10 cm above the soil surface). The chambers were constructed from polycarbonate (which is transparent to light of wavelengths above 420 nm) with a cross-section area ( $A$ ) of 0.066 m<sup>2</sup>, a height of 0.18 m, and thus giving a total volume of 11.8 L. Solenoid valves (model Galtek 203-3414-215, Entegris, USA) controlled the flow of sample air (4 L min<sup>-1</sup>) to the analyzers through blue-colored PTFE tubing. All fittings in contact with the sample air were constructed of TEFLON<sup>®</sup>.

[17] The concentrations of all trace gas species  $j$  inside the chambers ( $C(j)_{\text{chamber}}$ ) were measured sequentially for 3 min followed by 2 min of ambient air ( $C(j)_{\text{ambient}}$ ) measurements. Half a minute flush time was discarded prior to each measurement such that fluxes for each of the four chambers could be determined once every 24 min. Chamber fluxes ( $F(j)_{\text{chamber}}$ ) of each trace gas  $j$  were determined by mass balance,

$$F(j)_{\text{chamber}} = Q/A [C(j)_{\text{chamber}} - C(j)_{\text{ambient}}] \quad (j = \text{NO}, \text{NO}_2, \text{O}_3) \quad (2)$$

which accounted for the individual losses to the chamber walls, and gains and losses due to NO–NO<sub>2</sub>–O<sub>3</sub> reactions

within the air sample while passing through the dynamic chamber. A complete and detailed description of the flux evaluation procedure is given by Meixner *et al.* [1997].

[18] Uncertainty of the chamber flux measurements was determined by the sum of the errors due to nonstationarity (trend) in the ambient concentrations and to instrument drift/noise such that

$$\sigma(F(j)_{\text{chamber}}) = Q/A \left[ (\sigma(C(j)_{\text{trend}})^2 + 2(\sigma(C(j)_{\text{instrument}})^2) \right]^{1/2} \quad (3)$$

The trend related error  $\sigma(C(j)_{\text{trend}})$  in the data was quantified as half the absolute difference between ambient concentra-

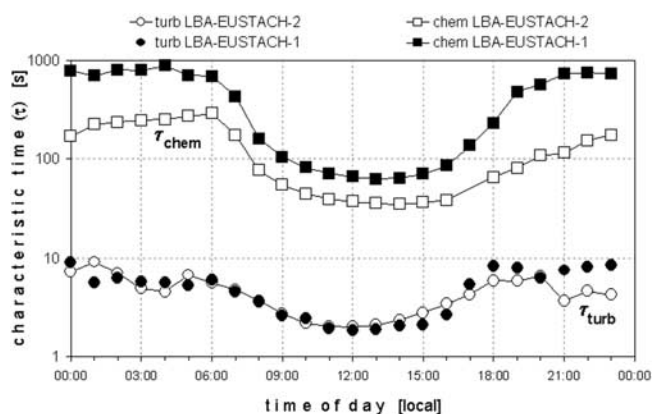


Figure 3. Chemical and turbulent characteristic timescales.

tions  $C(j)_{\text{ambient}}$  measured directly before and after the measurement of chamber air. It ranged 0–0.13 ppb for NO, 0–0.25 ppb for NO<sub>2</sub> and 0–2.9 ppb for O<sub>3</sub>. The standard deviation of all the zero air measurements, during calibration, was used for the determination of the instrument error  $\sigma(C(j)_{\text{instrument}})$  (Table 1). Thereafter flux data whose total error exceeded their magnitude or whose trend error exceeded the instrument error were removed in accordance with

$$(\sigma(F(j)_{\text{chamber}}) > |F(j)_{\text{chamber}}|) \text{ or } (\sigma(C(j)_{\text{trend}}) > \sigma(C(j)_{\text{instrument}})) \quad (4)$$

Due to power failures, instruments failure, and the above data rejection criteria, dynamic chamber flux data were reduced by more than 50% during LBA-EUSTACH-2 (cf. Figures 4, 5, 6, and 7).

[19] Chamber flux measurements were also accompanied by measurements of soil temperature, soil moisture, and soil surface wetness inside and outside the chambers (Table 1). Identical concurrent measurements were conducted at the EUSTACH forest site at *Reserva Biologica Jarú* (RBJ) 80 km NE of FNS [Gut et al., 2002a, 2002b].

#### 2.4. Inferential Method for Determination of NO<sub>2</sub> and O<sub>3</sub> Fluxes

[20] The emission flux of NO ( $F(\text{NO})_{\text{chamber}}$ ) as determined by the dynamic chamber system (above) is considered to be representative of actual field conditions. This holds true as NO consumption and emission processes are predominantly controlled by soil nutrients, diffusivity, moisture, and temperature [Davidson et al., 2000; Ludwig et al., 2001]. In contrast, dry deposition fluxes of NO<sub>2</sub> and O<sub>3</sub> depend on surface uptake characteristics, surface concentrations, and turbulent transfer conditions close to the surface. The design of the chamber and particularly the rapid exchange (2.4 times per minute) of the headspace air ensured that air temperature, relative humidity, and light intensity were close to ambient conditions [Ludwig, 1994; Meixner et al., 1997]. However, turbulent transfer conditions controlling the supply of trace gases to the surface may differ from conditions outside the chamber. Therefore chamber NO<sub>2</sub> and O<sub>3</sub> fluxes were not representative for ambient field conditions. In order to account for this difference, we applied an inferential method based on the “big leaf multiple resistance approach” [Wesely and Hicks, 1977; Hicks et al., 1997], where surface resistances inside and outside the chambers were assumed to be similar. The dry deposition flux  $F(j)$  of a nonreactive trace gas compound  $j$ , for which the surface represents a general sink at all ambient conditions, may be expressed as,

$$F(j) = C(j)/R_{\text{tot}}(j) \quad (5)$$

where  $C(j)$  is the ambient mixing ratio of the trace gas compound  $j$  at the reference height and  $R_{\text{tot}}(j)$  a gas transfer resistance in analogy to an electrical resistance according to Ohm’s law. Correspondingly,  $R_{\text{tot}}(j)$  is split into a series of partial resistances,

$$R_{\text{tot}}(j) = R_a + R_b + R_c(j) \quad (6)$$

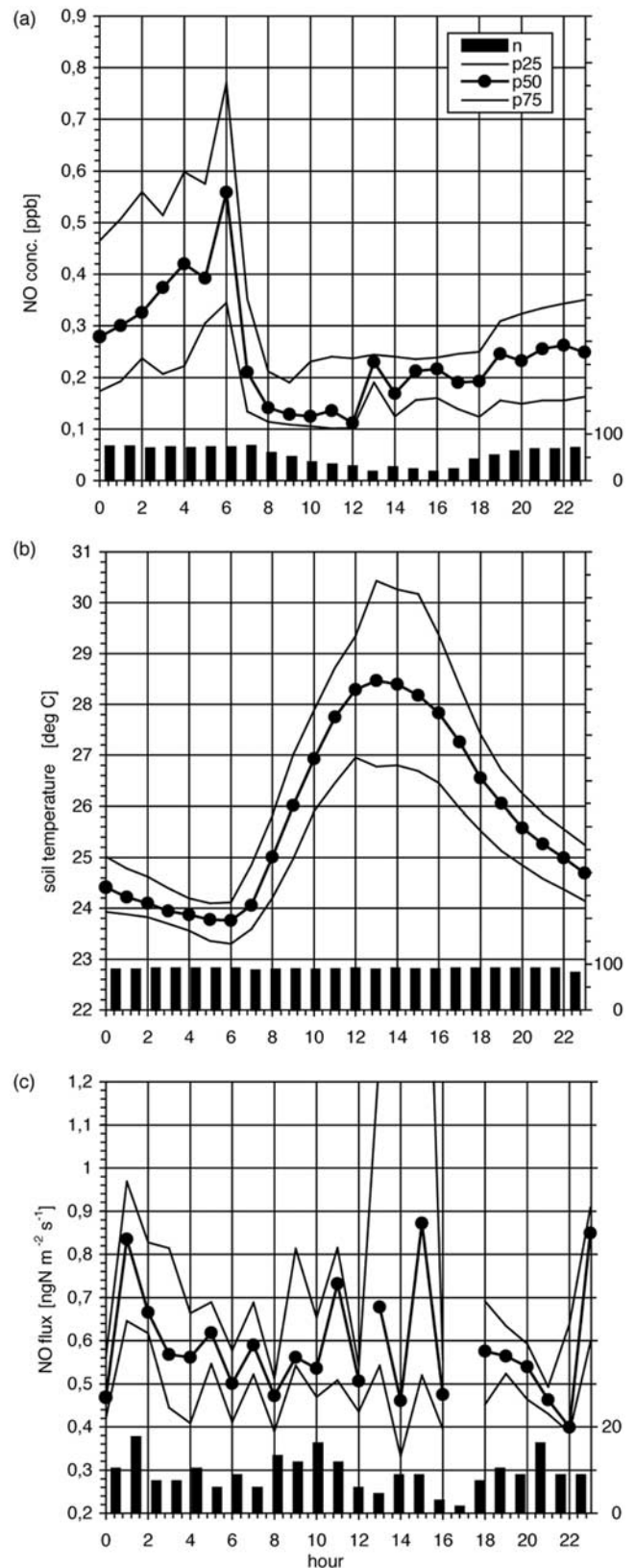


**Figure 4.** Mean diel variation of (a) NO concentration (ppb), (b) soil temperature (°C), and (c) soil NO emission flux ( $\text{ng N m}^{-2} \text{s}^{-1}$ ) at FNS for the dry-wet transition season during LBA-EUSTACH-2 (24 September to 27 October 1999). Bars indicate actual data counts used to derive the hour averages (solid points).

such that  $R_a$  is the resistance against turbulent exchange in the air; and  $R_b$  the molecular-turbulent boundary layer resistance close to the surface elements.  $R_c(j)$  is the canopy resistance of the trace gas compound  $j$  and comprises stomata, cuticle, soil, water, and other surface-related resistances. Due to the artificial ventilation of the chamber, the transport-related resistances (aerodynamic),  $R_a$  and  $R_b$ , differ from natural (outside) conditions, whereas the surface related resistance,  $R_c(j)$ , is the same inside and outside the chamber. Thus, for a transfer of chamber deposition measurements to representative natural conditions,  $R_a$  and  $R_b$  inside and outside the chamber must be quantified.

[21] The aerodynamic resistance inside the chamber ( $R_{\text{aero, chamber}}$ ), which is the sum of the turbulent resistance and molecular-turbulent boundary layer resistance inside the well-mixed chamber

$$R_{\text{aero, chamber}} = R_{\text{a, chamber}} + R_{\text{b, chamber}} \quad (7)$$

was determined experimentally [Galbally and Roy, 1980]. The soil surface enclosed by a dynamic chamber was replaced by a saturated potassium iodide (KI) solution, which represents a virtually ideal sink for ozone (i.e., its surface resistance to  $\text{O}_3$  uptake is virtually zero) [Ludwig, 1994]. Dividing the chamber  $\text{O}_3$  concentration by the flux (given by the flow rate through the chamber, the surface area of the KI solution, and the difference between ambient and chamber  $\text{O}_3$  concentrations according to equation (2)) yielded an  $R_{\text{aero, chamber}}$  of  $60 \text{ s m}^{-1}$ . Consequently the surface resistance for  $\text{NO}_2$  and  $\text{O}_3$  deposition in the chamber ( $R_c(\text{NO}_2)$  and  $R_c(\text{O}_3)$ ) was derived from the concentrations  $C(\text{NO}_2)_{\text{chamber}}$  and  $C(\text{O}_3)_{\text{chamber}}$ , the chamber fluxes  $F(\text{NO}_2)_{\text{chamber}}$  and  $F(\text{O}_3)_{\text{chamber}}$  such that

$$R_c(\text{NO}_2) = C(\text{NO}_2)_{\text{chamber}}/F(\text{NO}_2)_{\text{chamber}} - R_{\text{aero, chamber}} \quad (8a)$$

$$R_c(\text{O}_3) = C(\text{O}_3)_{\text{chamber}}/F(\text{O}_3)_{\text{chamber}} - R_{\text{aero, chamber}} \quad (8b)$$

[22] According to equation (6), the  $R_c$  has to be added to  $R_a$  and  $R_b$ , determined for ambient conditions outside the chamber, to yield representative values for  $R_{\text{tot}}(\text{NO}_2)$  and  $R_{\text{tot}}(\text{O}_3)$ . From FNS wind speed and air temperature profile data (cf. section 2.5), representative turbulent resistances ( $R_a$ ) and molecular-turbulent boundary layer resistances ( $R_b$ ) were estimated according to Hicks *et al.* [1987].  $R_a$  was determined using friction velocities ( $u_*$ ) and Monin–Obukhov lengths ( $L$ ) calculated using a generalized algorithm [Ammann, 1999] from wind speed and air temperature profiles such that

$$R_a = (k u_*)^{-1} [\ln(z_{\text{ref}}/z_0) - \Psi_c(z_{\text{ref}}/L)] \quad (9)$$

where the von Karmán constant ( $k$ ) was 0.4,  $z_0$  was the roughness length (LBA-EUSTACH-1: 0.15 m; LBA-EUSTACH-2: 0.11 m),  $z_{\text{ref}}$  was the reference height of 3.5 m, and  $\Psi_c(z_{\text{ref}}/L)$  is a function, which corrects for atmospheric nonneutral stability conditions [Ammann, 1999]. The molecular-turbulent boundary layer resistance ( $R_b$ ) is described by

$$R_b = (2/k u_*) (Sc/Pr)^p \quad (10)$$

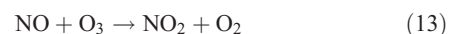
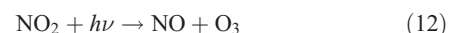
where the Schmidt number ( $Sc$ ) was 1.07 for the trace gases of interest, the Prandtl number ( $Pr$ ) was 0.72 and  $p$  was 2/3.

[23] Substitution of equations (8a), (8b), (9), and (10) into equation (6) gives  $R_{\text{tot}}(\text{NO}_2)$  and  $R_{\text{tot}}(\text{O}_3)$ . According to equation (5), ecosystem-wide dry deposition fluxes of  $F(\text{NO}_2)$  and  $F(\text{O}_3)$  were then calculated using the  $\text{NO}_2$  and  $\text{O}_3$  concentrations, which were measured at a reference height of 3.5 m above the surface of FNS (cf. section 2.2).

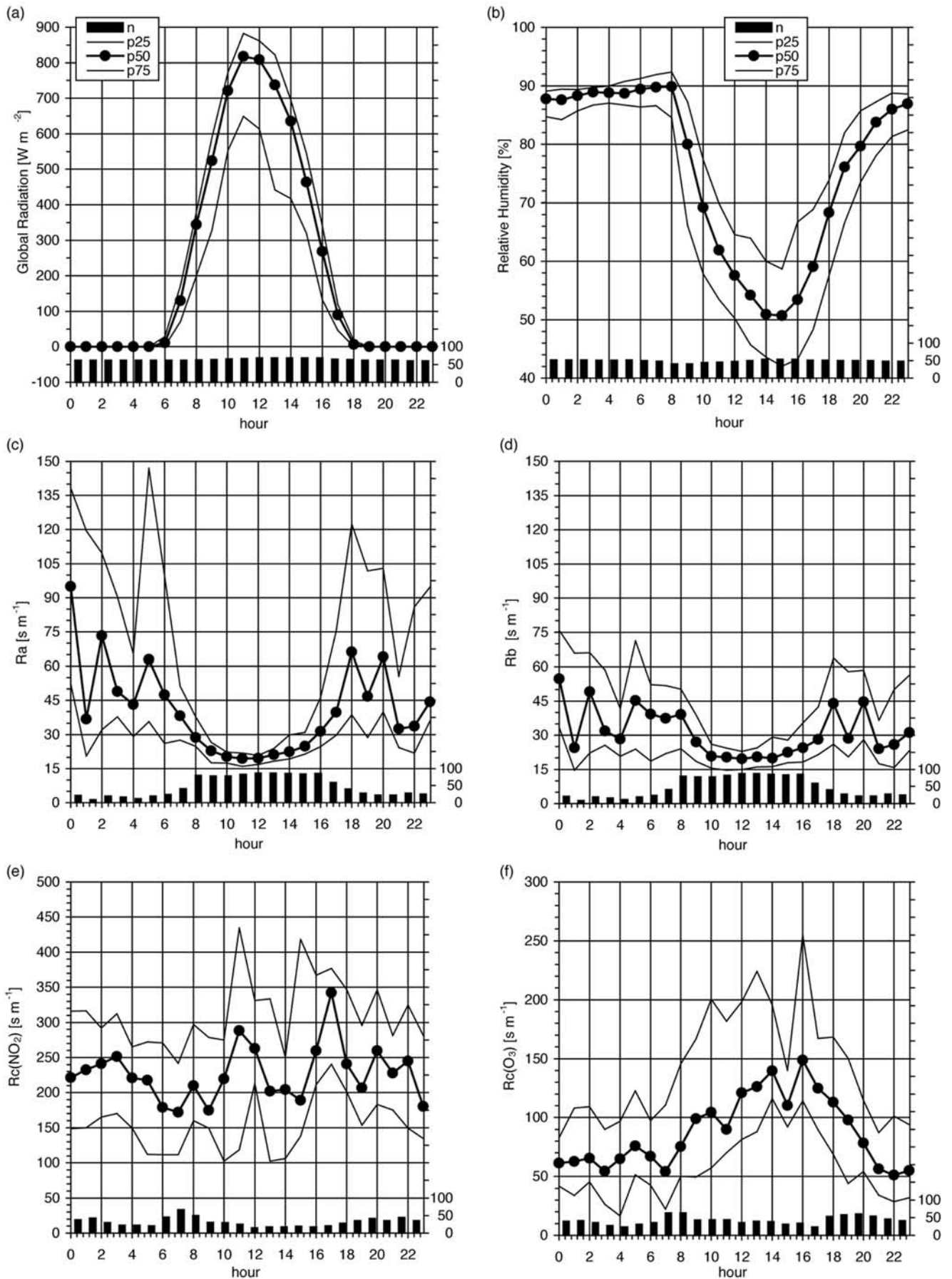
[24] As previously mentioned, the application of the inferential method is strictly valid for nonreactive trace gases only. An inferential method for reactive trace gases has to consider chemical reactions/transformations of these trace gases during the turbulent transport between the reference height and the surface [Kramm *et al.*, 1996]. However, the “nonreactive” flux–resistance relationship expressed by equation (5) can also be applied as a sufficient proxy in the case of reactive trace gases if “slow chemistry” is prevalent [Villá-Guerrau de Arellano and Duynderker, 1992] (i.e., if characteristic chemical reaction times are much larger than corresponding turbulent transport times). Following Villá-Guerrau de Arellano and Duynderker [1992], the characteristic time of turbulent transport ( $\tau_{\text{turb}}$ ) was calculated by

$$\tau_{\text{turb}} = k(z_{\text{ref}} + z_0)(\sigma_w^2/u_*^*)^{-1} \quad (11)$$

approximating  $\sigma_w/u_*$  by  $1.25 (1 - 3 z_{\text{ref}}/L)^{1/3}$  and  $1.25 (1 + 0.2 z_{\text{ref}}/L)$  for unstable and stable atmospheric conditions, respectively [Ammann, 1999]. The overall characteristic timescales for the  $\text{NO}-\text{NO}_2-\text{O}_3$  triad ( $\tau_{\text{chem}}$ ) are given by the combination [Lenschow, 1982] of  $\tau_{\text{NO}} = (k_{13} [\text{O}_3])^{-1}$ ,  $\tau_{\text{NO}_2} = k_{12}^{-1} = j(\text{NO}_2)^{-1}$ , and  $\tau_{\text{O}_3} = (k_{13} [\text{NO}])^{-1}$ , with the reaction constants  $k_{12} = j(\text{NO}_2)$  ( $\text{s}^{-1}$ ) and  $k_{13} = 2 \times 10^{-12} \exp(-1400/T)$  ( $\text{cm}^3 \text{ molecules}^{-1} \text{ s}^{-1}$ ) for the reactions,



The  $\text{NO}_2$  photolysis rate  $j(\text{NO}_2)$  was calculated from global radiation data (Table 1) using a relationship derived from simultaneous measurements of global radiation and the  $\text{NO}_2$  photolysis rate at RBJ during LBA-EUSTACH-1 and LBA-EUSTACH-2 (Ammann, C., U. Rummel, A. Gut, M. Scheibe, F. X. Meixner, and M. O. Andreae, Canopy reduction effect on nitric oxide emission from Amazonian rain forests, submitted to *J. Geophys. Res.*). Monitored  $\text{NO}$ ,  $\text{NO}_2$ , and  $\text{O}_3$  concentrations and micro-meteorological data (cf. sections 2.2 and 2.5) were used to calculate mean diel variations of  $\tau_{\text{turb}}$  and  $\tau_{\text{chem}}$  for the LBA-EUSTACH-1 and LBA-EUSTACH-2 periods. Turbulent transport times were generally found to be at least one order of magnitude faster than chemical reaction times (Figure 3). “Slow chemistry” between  $z_{\text{ref}} = 3.5$  m and the surface could therefore be assumed, justifying the application of equation (5) to infer  $\text{NO}_2$  and  $\text{O}_3$  dry deposition fluxes for conditions at FNS during LBA-EUSTACH-1 and LBA-EUSTACH-2.



## 2.5. Micrometeorological Gradient System

[25] Profiles of wind speed and air temperature were obtained from corresponding continuous measurements at four levels on a 5-m tall tripod mast, which was set up 15 m south of the dynamic chamber system and 25 m southeast of the NO, NO<sub>2</sub>, and O<sub>3</sub> monitoring intake system (Figure 1). Wind direction was measured at 4.5 m and global radiation at 2.02 m aboveground. Data acquisition and averaging (30 min) was performed by a micrologger (21X, Campbell Sci. Ltd., U.K.). Micrometeorological sensors and their precision are listed in Table 1. Profile data have been rejected for wind sectors 217–265° and 301–322°, for which substantial flow distortions for the profile measurements were observed due to instrument shelters and other nearby structures. A generalized algorithm by Ammann [1999] was used to infer surface roughness ( $z_0$ ), friction velocities ( $u^*$ ), Monin–Obukhov lengths ( $L$ ), and stability correction functions  $\Psi_c(z/L)$  necessary for the calculation of the resistances  $R_a$  and  $R_b$  (equations (9) and (10); cf. section 2.4). To account for conditions of very low wind speeds and/or high thermal stability (where atmospheric turbulence seldom exists and micrometeorological techniques fail), data were rejected for  $u^* < 0.025 \text{ m s}^{-1}$  and  $z_{\text{ref}}/L > 10$ . Stringent application of data rejection criteria reduced daytime (nighttime) data availability to 76% (17%) and 74% (21%) during the LBA-EUSTACH-1 and LBA-EUSTACH-2 periods, respectively.

[26] To determine the dry deposition O<sub>3</sub> flux from its vertical gradient, another O<sub>3</sub> analyzer (cf. Table 1) was used for the gradient system during LBA-EUSTACH-1 and LBA-EUSTACH-2 campaigns. This O<sub>3</sub> analyzer was cross-compared with the “monitoring” O<sub>3</sub> analyzer (cf. section 2.2) for a total of 96 hours on four different occasions and showed good agreement (within  $\pm 1$  ppb). For the determination of the vertical O<sub>3</sub> gradient, two 1/4 in. (6.35 mm) PTFE tubes of identical length (6.25 m) were installed with inlets at  $z_4 = 4.5$  m and  $z_1 = 0.52$  m aboveground. The two intake lines were switched, alternating every 3 min, by a stainless steel 3-way valve, which fed into the sample port of the analyzer equipped with a 47-mm PTFE filter ( $>2 \mu\text{m}$ ). One-minute flush time was discarded prior to each measurement. Every 30 min, means and standard deviations of O<sub>3</sub> concentrations from both levels were calculated by the micrologger routine. Thereafter, data where the observed standard deviation of the O<sub>3</sub> concentrations exceeded the magnitude of the gradient were removed. This procedure reduced daytime (nighttime) vertical O<sub>3</sub> gradient data to 38% (35%) and 41% (38%) during LBA-EUSTACH-1 and LBA-EUSTACH-2, respectively. The O<sub>3</sub> dry deposition flux was calculated by the aerodynamic flux–gradient relationship given by Müller *et al.* [1993] and Meixner [1994b].

[27] Subsequently, the total dry deposition resistance  $R_{\text{tot}}(\text{O}_3)$  was calculated according to equation (5) and the canopy resistance ( $R_c(\text{O}_3)$ ) was finally obtained (according to equation (6)) by subtracting  $R_a$  and  $R_b$ .

The latter were quantified by equations (9) and (10). Nighttime  $R_{\text{tot}}(\text{O}_3)$  data obtained by the micrometeorological technique were not considered for this study since the data rejection procedures on both micrometeorological and O<sub>3</sub> gradient data reduced these to less than 10% their original size.

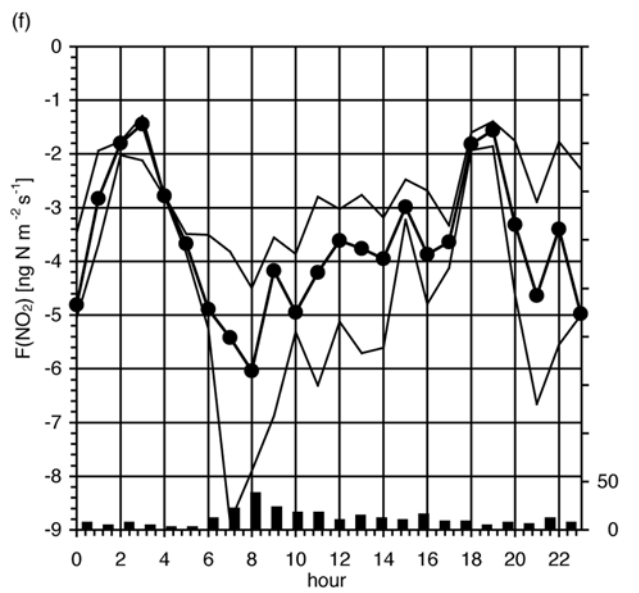
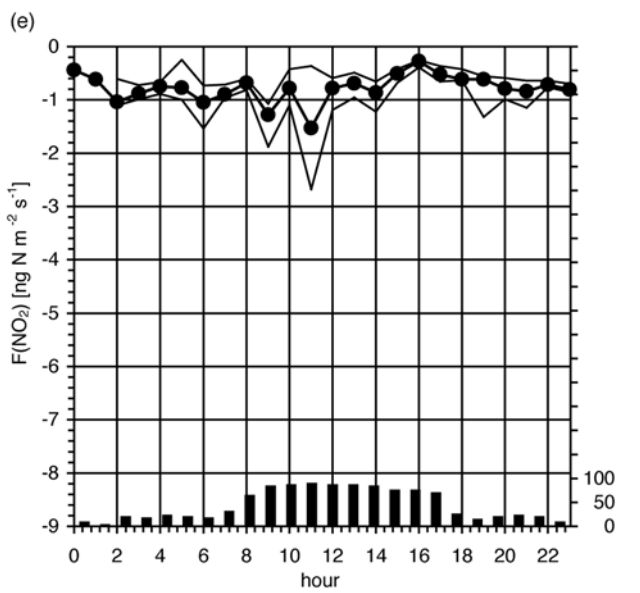
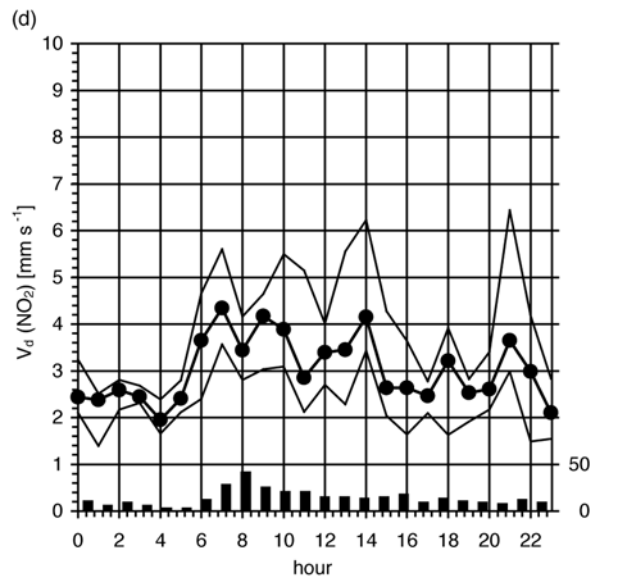
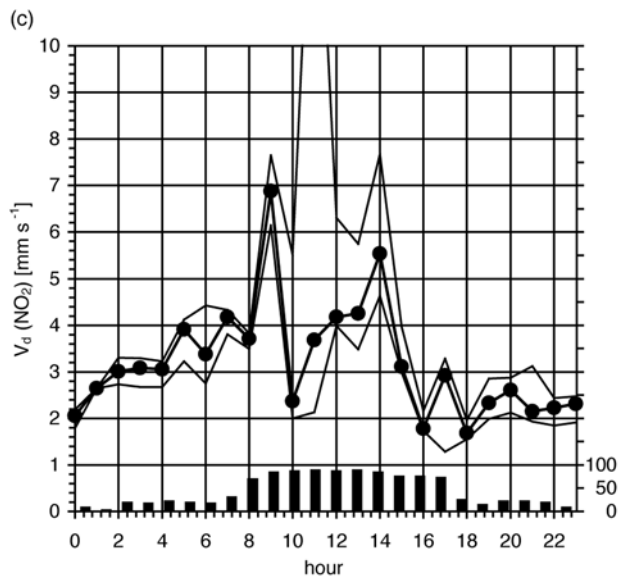
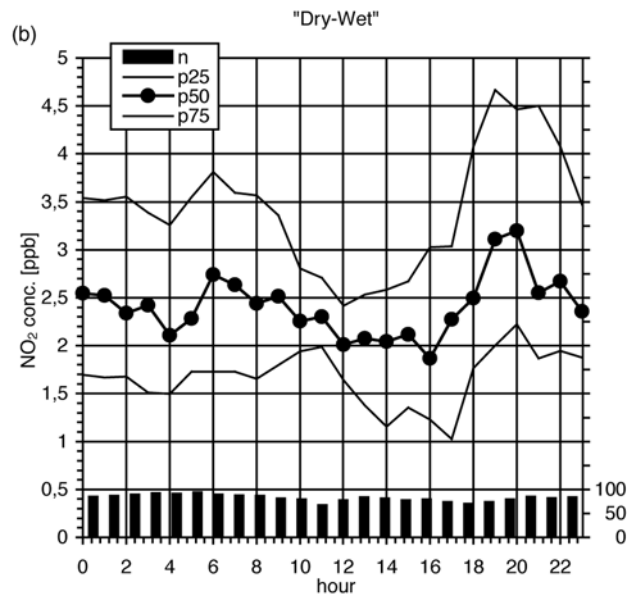
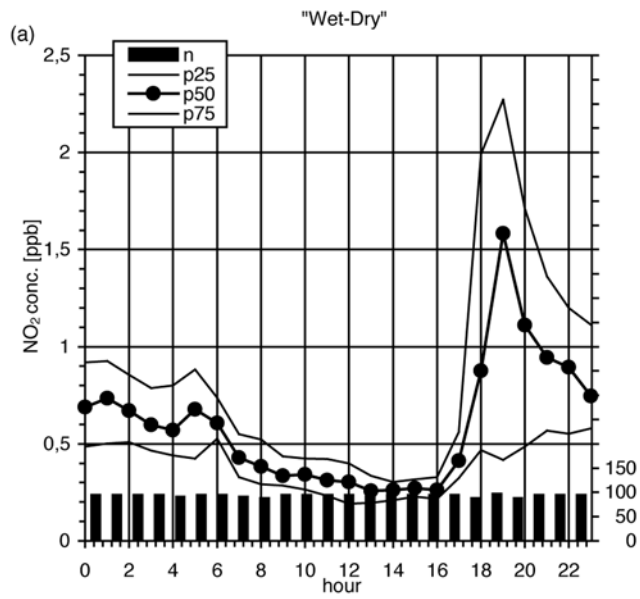
## 2.6. Determination of Soil Properties

[28] For the interpretation of the gas-exchange measurements, physical and chemical soil properties were determined for the measurement site. Soil diffusivity was determined by measurement of the naturally occurring transport tracer <sup>222</sup>Rn with a system identical to that used at *Reserva Biologica Jarú* [Gut *et al.*, 1999, 2002a]. It comprised a closed system of two 1-m gas permeable membrane tubes (Acurrel<sup>®</sup>) buried at 3 cm, a <sup>222</sup>Rn gas detector (Table 1), and a ventilated soil chamber. Determination of the soil bulk diffusion coefficient was estimated according to Fick’s first law using measurements of <sup>222</sup>Rn soil–atmosphere gradient and the <sup>222</sup>Rn surface flux [Gut *et al.*, 1998] at 10-min intervals for 3 days. The top 5 cm of soil from the chamber measurement site at FNS was analyzed for organic carbon, total phosphorous, total nitrogen, total sulfur, plant available phosphorous, potassium, pH (CaCl<sub>2</sub>), bulk density, texture, and cation exchange capacity in accordance with methods described by Emde and Szöcs [2000]. Determination of ammonium, nitrate, net mineralization, net nitrification, and potential nitrification rates were performed in accordance with methods described by Hart *et al.* [1994].

## 3. Results and Discussion

[29] In this section, time series data are presented as mean diel courses for reasons of compactness and simplicity. Furthermore, data were grouped into 1-hour intervals centered at the local time hour. Medians together with first and third quartiles were used to graphically present results for both measurements campaigns LBA-EUSTACH-1 (18 days) and LBA-EUSTACH-2 (34 days). For all trace gas fluxes, the micrometeorological convention of negative downward fluxes and positive upward direction has been adopted. As previously mentioned stringent data rejection criteria (detection limits, nonstationarities, and “low turbulence”) were applied to ensure data quality thereby reducing data counts by more than 50%. This is especially the case at night where 1-hour averages are derived from fewer than 10 data points. In this case “low turbulence” events result in these data being discarded (not possible to derive  $R_a$  and  $R_b$ ). Data counts are presented as bars in the Figures 4, 5, 6, and 7. Nevertheless, we felt it appropriate to supplement the presentation of the first measurements of the NO–NO<sub>2</sub>–O<sub>3</sub> exchange over a tropical pasture during two separate seasons by adding an annual mean estimate. This is justifiable given the paucity of similar measurements in this environment.

**Figure 5.** (opposite) Diel (a) global radiation ( $\text{W m}^{-2}$ ), (b) relative humidity (%), (c)  $R_a$  ( $\text{s m}^{-1}$ ), (d)  $R_b$  ( $\text{s m}^{-1}$ ), (e)  $R_c(\text{NO}_2)$  ( $\text{s m}^{-1}$ ), and (f)  $R_c(\text{O}_3)$  ( $\text{s m}^{-1}$ ) first, second, and third quartiles for the dry–wet transition season during LBA-EUSTACH-2 (24 September to 27 October 1999). Bars indicate actual data counts used to derive the hour averages (solid points).



### 3.1. Soil Emission of NO and Its Relation to Soil Properties

#### 3.1.1. NO Emission Fluxes

[30] As mentioned previously, NO soil fluxes were determined directly from dynamic chamber measurements during the LBA-EUSTACH-2 campaign (September–October 1999). A statistical summary of the observed results is given in Table 4 and average diel cycles are displayed in Figure 4. The minimum detectable NO emission flux was  $0.28 \text{ ng N m}^{-2} \text{ s}^{-1}$ . Soil moisture ranged from 19.5 to 70.7% WFPS with a mean of 35.7% WFPS. Soil temperature averaged  $25.5 \text{ }^\circ\text{C}$  and ranged between 19 and  $38 \text{ }^\circ\text{C}$  (Figure 4). The observed NO soil emissions were some of the lowest fluxes measured on an established pasture in the Amazon basin with a mean of  $0.65 \text{ ng N m}^{-2} \text{ s}^{-1}$  ( $\pm 0.37 \text{ ng N m}^{-2} \text{ s}^{-1}$ ). NO emission fluxes also showed no diel dependence on soil temperature and/or soil moisture WFPS ( $r^2 = 0.03$ ,  $\alpha = 0.05$ ; cf. Figure 4c). The pronounced early morning peak in ambient NO concentration measured at 10 cm aboveground (Figure 4a) was most likely due to photolysis of accumulated nighttime  $\text{NO}_2$  shortly after sunrise and is not a microbial response to increased surface wetness.

[31] Median NO emission fluxes at FNS were nine times lower than at the RBJ primary rain forest site under similar soil moisture and temperature conditions (see companion papers by Gut *et al.* [2002a, 2002b] and van Dijk *et al.* [2002]). We discuss below the possible physical and chemical soil factors (soil gas diffusion and nitrogen status) that explain the difference between the FNS and the RBJ sites.

#### 3.1.2. Soil Diffusivity

[32] Bulk density tends to increase with pasture age [Feigl *et al.*, 1995], which directly affects soil gas diffusion. Compaction through mechanized forest clearing, ploughing, seed drilling, and cattle hoof action results in an increase in soil bulk density, soil tortuosity, and thereby the length of time a NO gas molecule takes to diffuse through the soil profile. Thereby increasing the chance of utilization (consumption) of the gas by denitrifiers (M. Gödde and R. Conrad, Influence of soil properties on the turnover of nitric oxide and nitrous oxide by nitrification and denitrification at constant temperature and moisture, submitted to *Biology and Fertility of Soils*, 2000). Flux measurements and vertical profiles in soils have shown the half-life of NO to be in the order of minutes [Rudolph and Conrad, 1996]. The resultant emission flux is therefore a combination of NO production and consumption in the soil, which is largely soil diffusion dependant [Remde *et al.*, 1993]. Bulk density, for the top 5 cm of soil at FNS was  $1.56 \text{ Mg m}^{-3}$ , which was considerably higher (41%) than for the RBJ soil [Gut *et al.*, 2002a] and somewhat higher (16%) than for other pasture soils older than 20 years in Rondônia [Neill *et al.*, 1995, 1996, 1997, 1999; Feigl *et al.*, 1995; Kirkman, unpublished data, 1999]. This is similarly reflected in the NO effective diffusion coefficients measured at FNS,  $6.4 \pm 3.0 \times 10^{-7} \text{ m}^2 \text{ s}^{-1}$ , and at RBJ,  $7.9 \pm 4.0 \times 10^{-7} \text{ m}^2 \text{ s}^{-1}$ , for a range of soil–water conditions (10–20%) where

maximum NO production is expected (S. van Dijk and F. X. Meixner, Production and consumption of NO in forest and pasture soils from the Amazon basin: A laboratory study, submitted to *Water, Air, and Soil Pollution*, 2000, hereinafter referred to as van Dijk and Meixner, submitted manuscript, 2000). This represents a 23% difference in soil diffusion between the two sites and can be attributed to the higher bulk density and the relative absence of soil macro pores and soil fauna (termite and earthworm passages) at FNS (personal observation). However, this difference is too small to explain the observed difference in the NO emission flux between pasture and forest.

#### 3.1.3. Soil Nitrogen Status

[33] The repeated effects of slash-and-burn agriculture on tropical ecosystems are postulated to result in reduced overall soil N cycling and have been shown (cf. section 2.1) to result in lower productivity with time [Palm *et al.*, 1996]. Reduced bulk litter inputs result in poor N availability and a suppression of nitrification and mineralization [Piccolo *et al.*, 1994, 1996; Neill *et al.*, 1999]. This is partly manifested in the high soil C/N ratios (21:1) that were found at FNS.

[34] Inorganic ammonium pools ( $16.2 \text{ } \mu\text{g NH}_4^+ \text{ g}^{-1}$  soil or  $12.6 \text{ } \mu\text{g N-NH}_4^+ \text{ g}^{-1}$  soil) were a factor 10 larger than the inorganic nitrate pools ( $5.3 \text{ } \mu\text{g NO}_3^- \text{ g}^{-1}$  soil or  $1.2 \text{ } \mu\text{g N-NO}_3^- \text{ g}^{-1}$  soil). N pool sizes are considered to be reasonable indicators of soil nitrogen cycle dynamics, which suggests that FNS had a conservative rather than fast nitrogen soil turnover rate [Davidson *et al.*, 2000]. Nitrogen cycling of the soils at FNS showed similar characteristics to older pastures in Rondônia (Tables 2 and 3). Negative net mineralization ( $-0.89 \text{ } \mu\text{g NH}_4^+ \text{ g}^{-1}$  soil  $\text{d}^{-1}$ ) and the weak positive net nitrification rates ( $0.40 \text{ } \mu\text{g NO}_3^- \text{ g}^{-1}$  soil  $\text{d}^{-1}$ ) also suggest a large portion of the N turnover was immobilized by microbes [Hart *et al.*, 1994]. Potential nitrification rates indicate the maximum rate of  $\text{NH}_4^+$  oxidation by ammonium oxidizers [Besler, 1979] (Table 3), and rates at FNS ( $1.69 \text{ } \mu\text{g NO}_3^- \text{ g}^{-1} \text{ d}^{-1}$ ) were found to be within the upper ranges measured by Verchot *et al.* [1999] in Pará ( $0.18\text{--}1.70 \text{ } \mu\text{g NO}_3^- \text{ g}^{-1} \text{ d}^{-1}$ ) for active and degraded old pastures. They are, however, a factor three lower than those of forest and secondary forest soils (Kirkman, unpublished data, 1999), indicating that ammonia oxidizers are possibly restrained by conversion from forest to pasture [Verchot *et al.*, 1999]. The low NO emissions measured at FNS during September–October 1999 are assumed to be a combination of lower NO effective soil diffusion and a reduced N cycle. This is supported by field measurements of diffusion, a dominant inorganic ammonium nitrogen pool, and lower potential nitrification rates, corroborated by a site history of declining agricultural productivity. Established pastures in Rondônia may possess similar soil NO emission conditions.

### 3.2. Surface Resistances of $\text{NO}_2$ and $\text{O}_3$

[35] The measurement of daytime and nocturnal resistances has important implications for multiresistance modeling. Results presented here are among the first observations from

**Figure 6.** (opposite) Diel (a and b)  $\text{NO}_2$  concentrations (ppb), (c and d) deposition velocities ( $\text{mm s}^{-1}$ ), and (e and f) parameterized  $\text{NO}_2$  fluxes ( $\text{ng N m}^{-2} \text{ s}^{-1}$ ) first, second, and third quartiles for LBA-EUSTACH-1 and LBA-EUSTACH-2. Bars indicate actual data counts used to derive the hour averages (solid points).

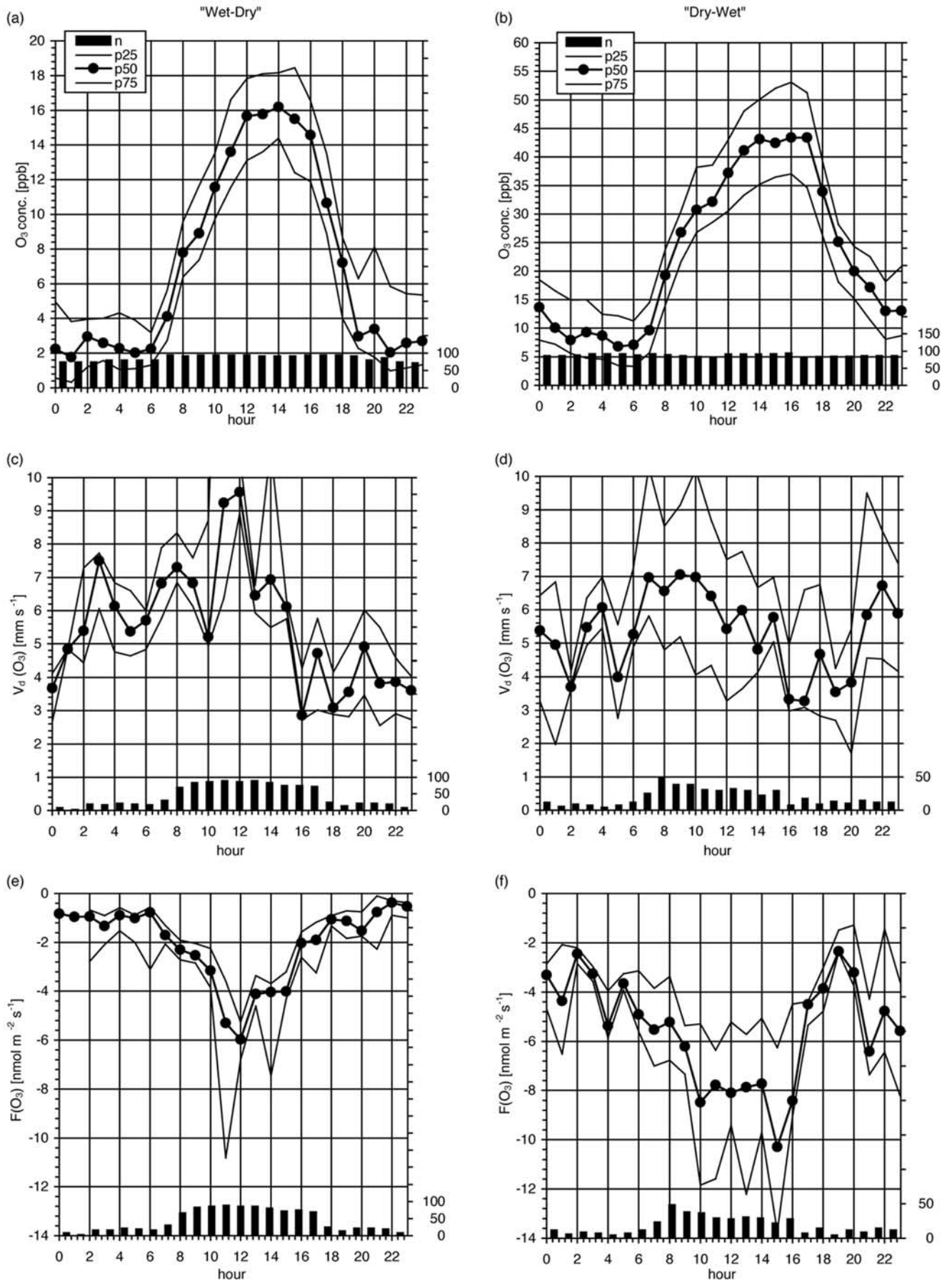


**Table 2.** Net Mineralization and Nitrification Rates for Established Pastures in Rondônia

Pasture (older than 20 yrs.)	$\mu\text{g NH}_4^+ \text{ g}^{-1} \text{ d}^{-1}$	$\mu\text{g NO}_3^- \text{ g}^{-1} \text{ d}^{-1}$
Neill <i>et al.</i> [1997] (Nova Vida)	-0.023	-0.02
Neill <i>et al.</i> [1999] (Nova Vida)	0.03	0.16
Neill <i>et al.</i> [1997] (Ouro Preto)	-0.22	0.22

a soil and grassland (*B. brizantha*) environment in the tropics where uptake resistances were measured on a 24-hour basis. Studies of  $\text{NO}_2$  and  $\text{O}_3$  uptake resistances over temperate grasslands are often limited to measurements during the day (e.g., for  $\text{NO}_2$  on lawn: 333–769  $\text{s m}^{-1}$  [Delany and Davies, 1983] and pasture: 38–67  $\text{s m}^{-1}$  [Duyzer *et al.*, 1983]). Rates of removal of  $\text{O}_3$  by grasslands have been reported by Pio *et al.* [2000] to be 500  $\text{s m}^{-1}$  at night to 200  $\text{s m}^{-1}$  during the day, and Massman *et al.* [1993] reported 100  $\text{s m}^{-1}$  over a semiarid grassland.

[36] Canopy resistance values ( $R_c(\text{NO}_2)$  and  $R_c(\text{O}_3)$ ) were measured by the dynamic chamber system during the LBA-EUSTACH-2 (dry–wet) campaign as described in section 2.3. In addition,  $R_a$  and  $R_b$  and a limited (daytime) data set of  $R_c$  values for  $\text{O}_3$  were determined from the aerodynamic gradient measurement system during both campaigns (cf. section 2.5). The corresponding median and IQR (interquartile range) for daytime and nighttime  $R_a$ ,  $R_b$ ,  $R_c$ , and  $v_d$  (deposition velocity in  $\text{mm s}^{-1}$ ) for  $\text{NO}_2$  and  $\text{O}_3$  are listed in Table 4. Diel resistance courses are presented together with global radiation and relative humidity for the dry–wet period in Figure 5.

[37] During LBA-EUSTACH-2 (dry–wet) median turbulent resistances ( $R_a$ ) were 23  $\text{s m}^{-1}$  during the day (0600–1800 LT) and 51  $\text{s m}^{-1}$  at night, whereas the day and night molecular-turbulent boundary layer resistances ( $R_b$ ) were 23  $\text{s m}^{-1}$  and 33  $\text{s m}^{-1}$ , respectively (Table 4). These near surface boundary layer resistance components ( $R_a$  and  $R_b$ ) followed a typical diel trend in accordance with increased turbulent mixing during daytime due to higher wind speeds and thermal convection (Table 4). However, these data only reflect the nights with relatively high wind speeds that passed the rejection criteria described in section 2.5. For the majority of the nighttime cases which did not pass the rejection procedure, much higher resistances have to be assumed, indicating a very weak or intermittent turbulence. Canopy resistances of both gases controlled the deposition processes during the day for both measurement periods and contributed more than 65% of the total resistance ( $R_a + R_b + R_c$ ). Day and night  $\text{NO}_2$  canopy resistance means, during LBA-EUSTACH-2, were significantly similar ( $\alpha = 0.05$ ) at 235  $\text{s m}^{-1}$  and 238  $\text{s m}^{-1}$  for day and night, respectively. Medians were 209  $\text{s m}^{-1}$  and 229  $\text{s m}^{-1}$  (Table 4). Ozone canopy resistances were significantly higher during daytime (106  $\text{s m}^{-1}$ ) than night 65  $\text{s m}^{-1}$  (Table 4). The highest  $\text{O}_3$  resistances (145  $\text{s m}^{-1}$ ) were observed at 1600 and at 1700 LT for  $\text{NO}_2$  (343  $\text{s m}^{-1}$ ) each day, which coincided with low relative humidity (Figure 5b), suggesting stomatal closure

due to high water vapor pressure deficit. The gradient and dynamic chamber derived  $R_c(\text{O}_3)$  values during the dry–wet period showed reasonable agreement, with daytime medians of 141  $\text{s m}^{-1}$  and 106  $\text{s m}^{-1}$ , respectively (Table 4). During LBA-EUSTACH-1 (wet–dry), nighttime conditions were even more stable and/or less turbulent, resulting in four times larger  $R_a$  and two times larger  $R_b$  nighttime values. Slightly lower  $R_a$  and  $R_b$  during the day were observed (Table 4), because of higher wind speeds [Andreae *et al.*, 2002]. Daytime total resistances, determined by the gradient method ( $R_a + R_b + R_c(\text{O}_3)$ ) for both the wet–dry and dry–wet periods also showed little seasonal difference, such that corresponding  $\text{O}_3$  deposition velocities ( $v_d(\text{O}_3) = R_{\text{tot}}(\text{O}_3)^{-1} = [R_a + R_b + R_c(\text{O}_3)]^{-1}$ ) were within 10% of each other during 1999 (Table 4).

[38] The diel patterns in  $\text{NO}_2$  and  $\text{O}_3$  resistances observed at FNS are considered to be the result of a combination of three processes: (1) stomatal, cuticular and mesophyll uptake, (2) soil uptake, and (3) uptake into solution of wet surfaces. The lower nighttime  $R_c(\text{O}_3)$ , when plant stomata are expected to be closed, is possibly due to a nighttime uptake of  $\text{O}_3$  via stomata and/or foliar cuticle [Kisser *et al.*, 1990] by the *B. brizantha* grass species. The similar daytime and nighttime  $R_c(\text{NO}_2)$  values indicates that the same holds true for  $R_c(\text{NO}_2)$ . However, during the day this stomatal activity gradually decreases with declining leaf water potential. At around 1600 LT when relative humidity was lowest, vapor pressure deficits were highest, causing partial stomatal closure and hence larger resistances [Pathre *et al.*, 1998]. This is in conflict with previous understanding that stomatal activity is typically higher during the day for  $C_4$  plants. However, a closer look at the dry and transition season (August–September 1992 and June 1993) data of McWilliam *et al.* [1996] suggests not much difference between the early and late part of the day. Unfortunately, night values were not measured (Roberts, personal communication, 2000). In addition, Jacob and Wofsy [1990] had to introduce an efficient nighttime mechanism in their model for  $\text{NO}_2$  plant uptake in order to balance their  $\text{NO}_y$  forest budget during ABLE-2B [Lerdau *et al.*, 2000]. A similar mechanism could be assumed for FNS. Soil uptake, on the other hand, is presumed to be diel invariant and a significant contributor to  $\text{NO}_2$  and  $\text{O}_3$  uptake at FNS. Soil has been shown to contribute as much as 75% to the total  $\text{O}_3$  depositional flux on Colorado semiarid grasslands [Massman, 1993], and ammonia oxidizers are thought to be significant consumers of  $\text{NO}_2$  [Zart and Bock, 1998; Schmidt and Bock, 1997].

[39] Surface wetness might also significantly alter the surface resistances of less soluble trace gases like  $\text{NO}_2$  and  $\text{O}_3$  [Baldochi, 1993; Chameides, 1987; Fuentes *et al.*, 1992; Schwartz, 1992; Wesely, 1989]. Surface moisture or condensation on soil and grass elements occurred mostly at night (>70% of all measurements of surface wetness) and was detectable by the wetness grids during 45% of all nights during LBA-EUSTACH-2 at FNS.  $\text{NO}_2$  and  $\text{O}_3$  resistances were 60 and 72% higher, respectively, during

**Figure 7.** (opposite) Diel (a and b)  $\text{O}_3$  concentrations (ppb), (c and d) deposition velocities ( $\text{mm s}^{-1}$ ), and (e and f)  $\text{O}_3$  fluxes ( $\text{nmol m}^{-2} \text{ s}^{-1}$ ) first, second, and third quartiles for LBA-EUSTACH-1 and LBA-EUSTACH-2. Bars indicate actual data counts used to derive the hour averages (solid points).

**Table 3.** Soil Properties for FNS, Determined During LBA-EUSTACH-2

Soil parameter	Value
Organic Carbon	1.87%
Total Phosphorus	0.021%
Total Nitrogen	0.122%
Total Carbon	2.58%
Total Sulfur	0.008%
Plant available Phosphorus	2.62 mg PO <sub>4</sub> 100 g <sup>-1</sup>
Plant available Potassium	13.04 mg K 100 g <sup>-1</sup>
pH [CaCl <sub>2</sub> ]	5.2
Bulk soil density	1.56 Mg m <sup>-3</sup>
Clay content	11.47%
Silt content	11.73%
Sand content	76.80%
Wilting Point <sup>a</sup>	6.69 cm <sup>3</sup> cm <sup>-3</sup>
Field Capacity <sup>a</sup>	19.56 cm <sup>3</sup> cm <sup>-3</sup>
CEC (cation exchange capacity)	16.77 mmol z <sup>-1</sup> 100g <sup>-1</sup>
Ammonium pool (NH <sub>4</sub> <sup>+</sup> )	16.81 μg NH <sub>4</sub> <sup>+</sup> g <sup>-1</sup>
Nitrate pool (NO <sub>3</sub> <sup>-</sup> )	5.25 μg NO <sub>3</sub> <sup>-</sup> g <sup>-1</sup>
Nitrite pool (NO <sub>2</sub> <sup>-</sup> )	0.27 μg NO <sub>2</sub> <sup>-</sup> g <sup>-1</sup>
Net mineralization rate	-0.89 μg NH <sub>4</sub> <sup>+</sup> g <sup>-1</sup> d <sup>-1</sup>
Net nitrification rate	0.40 μg NO <sub>3</sub> <sup>-</sup> g <sup>-1</sup> d <sup>-1</sup>
Potential nitrification rate	1.69 μg NO <sub>3</sub> <sup>-</sup> g <sup>-1</sup> d <sup>-1</sup>
C/N ratio	21.6

<sup>a</sup>Based on *Tomasella and Hodnett's* [1998] pedotransfer functions.

these wet nights as opposed to nights when no condensation occurred. Reports of enhanced O<sub>3</sub> deposition due to surface wetness have been noted above deciduous forests by *Fuentes et al.* [1992]. Their observations indicated that mechanisms other than stomatal uptake contributed to the O<sub>3</sub> deposition when the foliage was wet. Recent chemical models now make a distinction between foliage wetness caused by rain and dew to account for their different aqueous-phase chemical compositions [*Wesely*, 1989]. Therefore, nighttime  $R_c(\text{NO}_2)$  and  $R_c(\text{O}_3)$  values measured at FNS during the dry–wet period could be the competing result of plant, soil, and wet skin uptake (plant and soil) processes, accentuated by possible stomatal activity at

night and aqueous-phase chemistry on vegetative and soil surfaces. Moreover, the 24-h average canopy resistances for the pasture ( $R_c(\text{NO}_2) = 236$  and  $R_c(\text{O}_3) = 107$  s m<sup>-1</sup>), which comprised grass vegetation and soil, were 26 and 43% lower, respectively, than the forest floor ( $R_c(\text{NO}_2) = 319$  and  $R_c(\text{O}_3) = 188$  s m<sup>-1</sup>), comprising soil, root mat, and dead plant material at RBJ during the dry–wet season [*Gut et al.*, 2002b].

### 3.3. NO<sub>2</sub> and O<sub>3</sub> Deposition Fluxes and the NO<sub>x</sub> Budget at FNS Site

[40] In order to make a seasonal comparison of NO<sub>2</sub> and O<sub>3</sub> dry deposition fluxes at FNS, fluxes were calculated for both periods using the inferential method described in section 2. For LBA-EUSTACH-2, all day and night values of  $R_c(\text{NO}_2)$  and  $R_c(\text{O}_3)$  from the dynamic chambers were used, while for LBA-EUSTACH-1 only the daytime  $R_c(\text{O}_3)$  from the aerodynamic method were available directly. Unfortunately, number counts rendered nighttime  $R_c(\text{O}_3)$  calculated with the aerodynamic method nonsignificant (cf. section 2.5), and these data were substituted with  $R_c(\text{O}_3)$  measured by the dynamic chamber system during the dry–wet period. Correspondingly,  $R_c(\text{NO}_2)$  were estimated by

$$R_c(\text{NO}_2)_{\text{wet-dry}} = R_c(\text{O}_3)_{\text{wet-dry}} \left[ R_c(\text{NO}_2)_{\text{dry-wet}} / R_c(\text{O}_3)_{\text{dry-wet}} \right] \quad (14)$$

as an empirically adjusted first-order estimate of dry deposition flux for the wet–dry transition period. Diel NO<sub>2</sub> and O<sub>3</sub> concentrations and inferred diel NO<sub>2</sub> and O<sub>3</sub> dry deposition fluxes for both periods are presented in Figures 6 and 7. In addition, mean, standard deviation, count, and quartile statistics of NO<sub>2</sub> and O<sub>3</sub> dry deposition fluxes are given in Table 5.

[41] During LBA-EUSTACH-2, NO<sub>2</sub> and O<sub>3</sub> concentrations were considerably elevated above those measured

**Table 4.** Median and Interquartile Range (IQR) (s m<sup>-1</sup>) of Canopy Resistances  $R_c(\text{NO}_2)$  and  $R_c(\text{O}_3)$ , Turbulent Resistances  $R_a$ , Molecular-Turbulent Boundary Layer Resistances  $R_b$ ,  $v_d(\text{NO}_2) = R_{\text{tot}}(\text{NO}_2)^{-1}$  and  $v_d(\text{O}_3) = R_{\text{tot}}(\text{O}_3)^{-1}$  Deposition Velocities (mm s<sup>-1</sup>) for (a) LBA-EUSTACH-1 and (b) EUSTACH-2 Campaigns<sup>a</sup>

(a) LBA-EUSTACH-1, 30 April to 17 May 1999 wet–dry transition period									
	$R_a$		$R_b$		$R_c(\text{O}_3)^b$		$v_d(\text{O}_3)^b$		
	day	night	day	night	day	night	day	night	
median	20	79	22	54	100	(65) <sup>c</sup>	6	(5) <sup>c</sup>	
IQR	11	93	17	38	61	17	14	8	
(b) LBA-EUSTACH-2, 24 September to 27 October 1999 dry–wet transition period									
gas	$R_a$		$R_b$		$R_c$		$v_d$		
	day	night	day	night	day	night	day	night	
NO <sub>2</sub> (median)	23	51	23	33	209	229	4	3	
NO <sub>2</sub> (IQR)	13	76	16	41	182	149	6	6	
O <sub>3</sub> (median)	23	51	23	33	106	65	6	5	
O <sub>3</sub> (IQR)	13	76	17	41	101	50	8	7	
O <sub>3</sub> <sup>a</sup> (median)	23	51	23	33	141	–	5	–	
O <sub>3</sub> <sup>a</sup> (IQR)	13	76	17	41	130	–	6	–	

<sup>a</sup>Daily values fall between 0600 and 1800 LT. Values derived from substitution with values from the dry–wet period are in brackets.

<sup>b</sup>Aerodynamic gradient method for values between 0600 and 1800 LT.

<sup>c</sup>Values derived from substitution with dry–wet nighttime data.

**Table 5.** NO Emission Fluxes ( $\text{ng N m}^{-2} \text{s}^{-1}$ ), Dry Deposition Fluxes of  $\text{NO}_2$  ( $\text{ng N m}^{-2} \text{s}^{-1}$ ) and  $\text{O}_3$  ( $\text{nmol m}^{-2} \text{s}^{-1}$ ) Derived by the Inferential Method (cf. section 2.4) for LBA-EUSTACH-1 and LBA-EUSTACH-2 Campaigns: Means, Standard Deviations, Counts, Medians and Quartiles

(a) LBA-EUSTACH-1, 30 April to 17 May 1999 wet–dry transition period						
Gas	mean	std dev.	count %	Q25	median	Q75
$\text{NO}_2^{\text{a}}$	−0.91	0.89	46%	−1.05	−0.70	−0.46
$\text{O}_3^{\text{b}}$	−3.39	2.78	46%	−4.34	−2.75	−1.67
(b) LBA-EUSTACH-2, 24 September to 27 October 1999 dry–wet transition period						
Gas	mean	std dev.	count %	Q25	median	Q75
NO	0.65	0.39	9%	0.43	0.55	0.75
$\text{NO}_2$	−4.60	2.91	12%	−5.75	−3.93	−2.80
$\text{O}_3$	−6.76	4.07	19%	−8.74	−6.11	−3.71

<sup>a</sup> Values derived from a proxy  $R_c(\text{NO}_2)$  (cf. section 3.3).

<sup>b</sup> Values derived from substitution with dry–wet nighttime data.

during LBA-EUSTACH-1 at FNS. This can be attributed to biomass burning from forest clearing activities, which typically occur in the later part of the dry season [Andreae *et al.*, 2002]. Nitrogen dioxide concentrations were a factor three higher during the dry–wet transition season (Figure 6) resulting in deposition fluxes six times larger than those of the wet–dry period (−3.93 versus −0.7  $\text{ng N m}^{-2} \text{s}^{-1}$ ) (Table 5). An early evening peak in the  $\text{NO}_2$  concentration (more pronounced during the wet–dry period) was observed at ca. 1900 LT during both measurement periods. This peak was due to local advection of moderately aged pollution plumes (from nearby vehicular traffic along the RO-47) dispersing in a very shallow, stable, and young nocturnal boundary layer [Meixner *et al.*, 2000]. Ozone concentrations were equally elevated during the dry–wet period with deposition  $F(\text{O}_3)$  fluxes twice as large (−6.11  $\text{nmol m}^{-2} \text{s}^{-1}$  or 0.13  $\mu\text{g m}^{-2} \text{s}^{-1}$ ) during the dry–wet in contrast to the fluxes (−2.75  $\text{nmol m}^{-2} \text{s}^{-1}$  or 0.29  $\mu\text{g m}^{-2} \text{s}^{-1}$ ) during the wet–dry season. Since resistance conditions are similar through the year (cf. section 3.2), consideration of seasonal ambient  $\text{O}_3$  trace gas conditions is vital for quantifying the deposition of  $\text{O}_3$  at expanded spatial and temporal scales in the Amazon basin. Assuming that measurements during LBA-EUSTACH-1 and LBA-EUSTACH-2 were representative for both wet and dry seasons and that these seasons were equal in length, the mean  $\text{O}_3$  dry deposition was  $0.24 \pm 0.013 \mu\text{g m}^{-2} \text{s}^{-1}$ . This is slightly higher than the  $0.19 \mu\text{g m}^{-1} \text{s}^{-1}$  first suggested as a mean for Amazonian pastures by Sigler *et al.* (J. M. Sigler, J. D. Fuentes, R. C. Heitz, and M. Garstang, Ozone dynamics and deposition processes at a deforested site in the Amazon basin, submitted to *Ambio*, 2000) on the basis of measurements for the 1999 wet season (January and February 1999 only) at FNS.

[42] NO soil emission fluxes were shown above to be extremely low (cf. section 3.1; Table 4) during the dry–wet period (0.65  $\text{ng N m}^{-2} \text{s}^{-1}$ ). Due to higher soil moisture in the wet season, which limits NO production and inhibits soil diffusion (van Dijk and Meixner, submitted manuscript, 2000), it is reasonable to assume that NO fluxes were similar or perhaps slightly lower during the dry–wet period. In this case, emission of NO and dry deposition of  $\text{NO}_2$  would be approximately equal during the wet–dry season (Table 5). However, during the dry–wet season, the surface of FNS removed up to seven times more  $\text{NO}_2$  from the atmosphere than was emitted as NO. Assuming, despite the low data

counts, that measurements during LBA-EUSTACH-1 and LBA-EUSTACH-2 were representative for the wet and dry seasons and that these seasons are about equal in length, this constitutes a net  $\text{NO}_2$  sink of  $0.73 \text{ kg N ha}^{-1} \text{ yr}^{-1}$ , which is a factor four larger than the NO emitted from the soil ( $0.17 \text{ kg N ha}^{-1} \text{ yr}^{-1}$ ) at FNS. Therefore FNS could be considered as a net  $\text{NO}_x$  ( $\text{NO}_x = \text{NO} + \text{NO}_2$ ) sink during 1999.

#### 4. Conclusion

[43] Rondônia, Brazil has in recent times undergone rapid replacement of natural forest by cleared land for commercial and small-scale agriculture. These agricultural areas typically decline in productivity within a relatively short period (2–6 yrs) after deforestation and are then either abandoned or planted to grass. Measurements of (1) NO fluxes, (2)  $\text{NO}_2$  and  $\text{O}_3$  canopy resistances, (3) and  $\text{NO}_2$  and  $\text{O}_3$  fluxes were conducted for two seasons (wet–dry and dry–wet) on the 22-year-old cattle pasture *Fazenda Nossa Senhora Aparecida* in the state of Rondônia, Brazil. The pattern of declining productivity found on old pastures was corroborated by the low NO flux emissions measured during the 1999 dry–wet season. During this season the pasture was shown to be a significant net  $\text{NO}_x$  sink, with elevated  $\text{NO}_2$  mixing ratios during the dry–wet season when biomass burning was most prevalent. There was little seasonal variation in the  $\text{NO}_2$  and  $\text{O}_3$  deposition velocities determined in the wet–dry and dry–wet seasons at FNS. However, deposition fluxes were a factor six larger during the dry–wet season. These observations indicate that ambient concentrations largely control dry deposition of  $\text{NO}_2$  and  $\text{O}_3$  over established pastures.

[44] The measurements of canopy resistances over FNS, which comprised of soil and vegetation (live and dead grass), revealed that these resistances controlled the larger nighttime uptake of  $\text{NO}_2$  and  $\text{O}_3$  during the two transition seasons in 1999. The combined plant, soil, and wet surface uptake of trace gases, accentuated by stomatal activity and aqueous phase chemistry on vegetative and soil surfaces at night, are believed to result in a trace gas deposition diel pattern only previously observed by Kaplan *et al.* [1988] near Manaus and by Andreae *et al.* [1992] in the Congo Basin. Their results (presented as deposition velocities) could not be explained by changes in stomatal activity alone and were put down to differences in the aerodynamic resistance ( $R_a$ ) component between the dry and wet seasons.

Further work on forest canopy and pasture soil and plant surface NO<sub>2</sub> and O<sub>3</sub> uptake processes is required to understand the diel pattern of canopy resistances observed in this study.

[45] **Acknowledgments.** The authors wish to thank the owner of *Fazenda Nossa Senhora Aparecida*, Afonso Pereira de Andrade, for the use of his land. The staff of Instituto Nacional de Colonização e Reform Agrária (INCRA) in Ji-Paraná, Rondônia, especially Jaõ Luis Esteves, Eduardo Conceição de Lacerda, and Claudionor Rodrigues, for their assistance during the field experiments. The staff of the Instituto Brasileiro do Meio Ambiente e dos Recursos Naturais Renováveis (IBAMA) in Ji-Paraná, Rondônia, for their assistance in the forest. P. Bahrmann for assistance with the soil analyses. This work was conducted with the financial support of the Graduate College *Kreisläufe, Austauschprozesse und Wirkungen von Stoffen in der Umwelt* (Gutenberg University, Mainz, Germany), the European Commission under the project EUSTACH-LBA, and the Max Planck Society, Germany.

## References

- Ammann, C., On the applicability of relaxed eddy accumulation and common methods for measuring trace gas fluxes, in *Zürcher Geographische Schriften*, p. 73, ETH, Zurich, 1999.
- Andreae, M. O., A. Chapuis, B. Cros, J. Fontan, G. Helas, C. Justice, Y. J. Kaufman, A. Minga, and D. Nganga, Ozone and Aitken nuclei over equatorial Africa: Airborne observations during DECAFE 88, *J. Geophys. Res.*, **97**, 6137–6148, 1992.
- Andreae, M. O., et al., Biogeochemical cycling of carbon, water, energy, trace gases and aerosols in Amazonia: The LBA-EUSTACH experiments, *J. Geophys. Res.*, **107**, 10.1029/2001JD00324, in press, 2002.
- Baldocchi, D. D., Deposition of gaseous sulfur compounds to vegetation, in *Sulfur Nutrition and Assimilation and Higher Plants*, edited by L. J. De Kok et al., pp. 271–293, SPB Acad., The Hague, Netherlands, 1993.
- Baumgartner, M., E. Bock, and R. Conrad, Processes involved in uptake and release of nitrogen-dioxide from soil and building stones into the atmosphere, *Chemosphere*, **24**, 1943–1960, 1992.
- Besler, L. W., Population ecology of nitrifying bacteria, *Annu. Rev. Microbiol.*, **33**, 309–333, 1979.
- Browder, J. O., and B. J. Godfrey, *Rainforest Cities*, 429 pp., Columbia Univ. Press, New York, 1997.
- Cardenas, L., A. Rondon, C. Johansson, and E. Sanhueza, Effects of soil moisture, temperature and inorganic nitrogen on nitric oxide emissions from acidic tropical savannah soils, *J. Geophys. Res.*, **98**, 14,783–14,790, 1993.
- Chameides, W. L., Acid dew and the role of chemistry in the dry deposition of reactive gases to wetted surfaces, *J. Geophys. Res.*, **92**, 11,895–11,908, 1987.
- Crutzen, P. J., Ozone in the troposphere, in *Composition, Chemistry, and Climate of the Atmosphere*, edited by H. B. Signh, Van Nostrand Reinhold, New York, 1995.
- Davidson, E. A., Sources of nitric oxide and nitrous oxide following wetting of dry soil, *Soil Sci. Soc. Am. J.*, **56**, 95–102, 1992.
- Davidson, E. A., M. Keller, H. E. Erickson, L. V. Verchot, and E. Veldkamp, Testing a conceptual model of soil emissions of nitrous and nitric oxides, *BioScience*, **50**, 667–680, 2000.
- Delany, A. C., and T. D. Davies, Dry deposition of NO<sub>x</sub> to grass in rural East Anglia, *Atmos. Environ.*, **17**, 1391–1394, 1983.
- Duyzer, J. H., G. M. Meyer, and R. M. Van Aalst, Measurement of dry deposition velocities of NO, NO<sub>2</sub> and O<sub>3</sub> and the influence of chemical reactions, *Atmos. Environ.*, **17**, 2117–2120, 1983.
- Emde, K., and A. Szöcs, Geoökologische arbeitsmethoden II, Johannes Gutenberg Univ., Mainz, 2000.
- Fehsenfeld, F. C., et al., A ground-based intercomparison of NO, NO<sub>x</sub>, and NO<sub>y</sub> measurements techniques, *J. Geophys. Res.*, **92**, 14,710–14,722, 1987.
- Feigl, B., J. Melillo, and C. C. Cerri, Changes in the origin and quality of soil organic matter after pasture introduction in Rondônia (Brazil), *Plant Soil*, **175**, 212–229, 1995.
- Fernando, G. W. E., Preliminary studies on the association of growth of grasses and legumes, *Trop. Agric. (Ceylon)*, **117**, 167–179, 1961.
- Fuentes, J. D., T. J. Gillespie, G. den Hartog, and H. H. Neumann, Ozone deposition onto a deciduous forest during dry and wet conditions, *Agric. For. Meteorol.*, **62**, 1–18, 1992.
- Galbally, I. E., and C. R. Roy, Destruction of ozone at the earth's surface, *Q. J. R. Meteorol. Soc.*, **106**, 599–620, 1980.
- Garcia-Montiel, D. C., P. A. Steudler, M. C. Piccolo, J. M. Melillo, C. Neill, and C. C. Cerri, Controls on soil nitrogen oxide emissions from forest and pastures in the Brazilian Amazon, *Global Biogeochemical Cycles*, **15**(4), 10.1029/2000GB001349, 2002.
- Gut, A., A. Blatter, M. Fahrmi, B. E. Lehmann, A. Neftel, and T. Staffelbach, A new membrane tube technique (METT) for continuous gas measurements in soils, *Plant Soil*, **198**, 87–97, 1998.
- Gut, A., A. Neftel, T. Staffelbach, M. Riedo, and B. E. Lehmann, Nitric oxide flux from soil during the growing season of wheat by continuous measurements of the NO soil–atmosphere concentration gradient: A process study, *Plant Soil*, **216**, 165–180, 1999.
- Gut, A., S. M. van Dijk, M. Scheibe, U. Rummel, M. Welling, C. Ammann, F. X. Meixner, M. O. Andreae, and B. E. Lehmann, NO emission from an Amazonian rain forest soil: Continuous measurements of NO flux and soil concentration, *J. Geophys. Res.*, **107**(X), 10.1029/2001JD000521, in press, 2002a.
- Gut, A., et al., Exchange fluxes of NO<sub>2</sub> and O<sub>3</sub> at soil and leaf surfaces in an Amazonian rainforest, *J. Geophys. Res.*, **107**(X), 10.1029/2001JD000654, in press, 2002b.
- Hart, S. C., J. M. Stark, E. A. Davidson, and M. K. Firestone, Nitrogen mineralization, immobilization and nitrification, in *Methods of Soil Analysis, part 2, Microbial and Biogeochemical Properties*, edited by R. W. Weaver et al., pp. 985–1018, Soil Sci. Soc. of Am., Madison, Wis., 1994.
- Hicks, B. B., D. D. Baldocchi, T. P. Meyers, R. P. Hosker Jr., and D. R. Matt, A preliminary multiple resistance routine for deriving dry deposition velocities from measured quantities, *Water Air Soil Pollut.*, **36**, 311–330, 1987.
- Hodnett, M. G., M. D. Oyama, J. Tomasella, and A. O. de Marques Filho, Comparisons of long-term soil water storage behavior under pasture and forest in three areas of Amazonia, in *Amazonian Deforestation and Climate*, edited by J. H. Gash, C. A. Nobre, J. M. Roberts, and R. L. Victoria, pp. 55–77, John Wiley, New York, 1996.
- Jacob, D. J., and S. C. Wofsy, Budgets of reactive nitrogen, hydrocarbons, and ozone over the Amazon forest during the wet season, *J. Geophys. Res.*, **95**, 16,737–16,754, 1990.
- Kaplan, W. A., S. C. Wofsy, M. Keller, and J. M. da Costa, Emission of NO and deposition of O<sub>3</sub> in a tropical forest system, *J. Geophys. Res.*, **93**, 1389–1395, 1988.
- Kisser, G., D. Bieniek, and H. Ziegler, NO<sub>2</sub> binding to defined phenolics in the plant cuticle, *Naturwissenschaften*, **77**, 492–493, 1990.
- Kolar, J., *Stickoxide und Luftreinhaltung*, Springer-Verlag, New York, 1990.
- Kramm, G., H. Müller, D. Fowler, K. D. Höfken, F. X. Meixner, and E. Schaller, A modified profile method for determining the vertical fluxes of NO, NO<sub>2</sub>, ozone and HNO<sub>3</sub> in the atmospheric surface layer, *J. Atmos. Chem.*, **13**, 265–288, 1991.
- Kramm, G., N. Beier, T. Foken, H. Müller, P. Schröder, and W. Seiler, A SVAT scheme for NO, NO<sub>2</sub> and O<sub>3</sub>: Model descriptions and test results, *Meteorol. Atmos. Phys.*, **61**, 89–106, 1996.
- Lenschow, D. H., Reactive trace species in the boundary layer from a micrometeorological perspective, *J. Meteorol. Soc. Jpn.*, **60**, 161–172, 1982.
- Lerdau, M. T., W. J. Munger, and D. Jacob, The NO<sub>2</sub> flux conundrum, *Science*, **289**, 2291–2293, 2000.
- Ludwig, J., Untersuchungen zum Austausch von NO und NO<sub>2</sub> zwischen Atmosphäre und Biosphäre, Dissertation, Fakul. Biol. Chem. Geowissenschaften, Univ. Bayreuth, Germany, 1994.
- Ludwig, J., F. X. Meixner, B. Vogel, and J. Förstner, Processes, influencing factors, and modeling of nitric oxide surface exchange: An overview, *Biogeochemistry*, in press, 2001.
- Massman, W. J., Partitioning ozone fluxes to sparse grass and soil and the inferred resistance to dry deposition, *Atmos. Environ.*, **27**, 167–174, 1993.
- McWilliam, A.-L. C., O. M. R. Cabral, B. M. Gomes, J. L. Esteves, and J. M. Roberts, Forest and pasture leaf-gas exchange in south-west Amazonia, in *Amazonian Deforestation and Climate*, edited by J. H. C. Gash, C. A. Nobre, J. Roberts, and R. L. Victoria, pp. 265–286, John Wiley, New York, 1996.
- Meixner, F. X., Surface exchange of odd nitrogen oxides, *Nova Acta Leopold.*, **70**(288), 299–348, 1994a.
- Meixner, F. X., Surface exchange of ammonia: Three different micrometeorological procedures applied, in *Physico-Chemical Behavior of Atmospheric Pollutants*, edited by G. Angeletti and G. Restelli, pp. 749–754, Report EUR 15609, Office for Official Publications of the European Communities 1994-XVIII (628 pp.), Luxembourg, 1994b (ISBN 92-826-7922-5).
- Meixner, F. X., Th. Fickinger, L. Marufu, D. Serca, F. J. Nathaus, E. Makina, L. Mukumbira, and M. O. Andreae, Preliminary results on nitric oxide emission from a southern African savanna ecosystem, *Nutr. Cycling. Agroecosyst.*, **48**, 123–138, 1997.
- Meixner, F. X., L. V. Gatti, G. A. Kirkman, A. M. Cordoba-Leal, M. L. Moura, E. Oliveira dos Santos, and M. O. Andreae, Surface mixing ratios

- of NO, NO<sub>x</sub>, and ozone at a west Amazonian pasture site during the 1999 wet-to-dry and dry-to-wet-transition periods, *Newsl. Eur. Geophys. Soc.*, **74**, 221, 2000.
- Moran, E. F., Deforestation and land use in the Brazilian Amazon, *Hum. Ecol.*, **2**, 1–21, 1993.
- Müller, H., F. X. Meixner, G. Kramm, D. Fowler, G. J. Dollard, and M. Possanzini, Determination of HNO<sub>3</sub> deposition by modified Bowen ratio and aerodynamic profile techniques, *Tellus*, **45B**, 346–367, 1993.
- Neill, C., M. C. Piccolo, P. A. Steudler, J. M. Melillo, B. J. Feigl, and C. C. Cerri, Nitrogen dynamics in soils of forests and active pastures in the western Brazilian Amazon basin, *Soil Biol. Biochem.*, **27**, 1167–1175, 1995.
- Neill, C., M. C. Piccolo, B. Fray, J. M. Melillo, P. A. Steudler, J. F. L. Moraes, and C. C. Cerri, Forest- and pasture-derived carbon contributions to carbon stocks and microbial respiration of tropical pasture soils, *Oecologia*, **107**, 113–119, 1996.
- Neill, C., M. C. Piccolo, C. C. Cerri, P. A. Steudler, J. M. Melillo, and M. Brito, Net nitrogen mineralization and net nitrification rates in soils following deforestation for pasture across the southwestern Brazilian Amazon basin landscape, *Oecologia*, **110**, 243–252, 1997.
- Neill, C., M. C. Piccolo, J. M. Melillo, P. A. Steudler, and C. C. Cerri, Nitrogen dynamics in Amazon forest and pasture soils measured by N-15 pool dilution, *Soil Biol. Biochem.*, **31**, 567–572, 1999.
- Palm, C. A., M. J. Swift, and P. L. Woerner, Soil biological dynamics in slash-and-burn agriculture, *Agric. Ecosyst. Environ.*, **58**, 61–74, 1996.
- Pathre, U., A. K. Sinha, P. A. Shirke, and P. V. Sane, Factors determining the midday depression of photosynthesis in trees under monsoon climate, *Trees*, **12**, 472–481, 1998.
- Piccolo, M. C., C. Neill, J. M. Melillo, and C. C. Cerri, <sup>15</sup>N Natural abundance in soils along forest–pasture chronosequences in the western Brazilian Amazon basin, *Oecologia*, 112–117, 1994.
- Piccolo, M. C., C. Neill, C. C. Cerri, and P. A. Steudler, N-15 natural abundance in forest and pasture soils of the Brazilian Amazon basin, *Plant Soil*, **182**, 249–258, 1996.
- Pio, C. A., M. S. Feliciano, A. T. Vermeulen, and E. C. Sousa, Seasonal variability of ozone dry deposition under southern European climate conditions in Portugal, *Atmos. Environ.*, **34**, 195–205, 2000.
- Remde, A., and R. Conrad, Role of nitrification and denitrification for NO metabolism, *Biogeochemistry*, **12**, 189–205, 1991.
- Remde, A., F. Slemr, and R. Conrad, Microbial production and uptake of nitric oxide in soil, *FEMS Microbiol. Ecol.*, **62**, 221–230, 1989.
- Remde, A., J. Ludwig, F. X. Meixner, and R. Conrad, A study to explain the emission of nitric oxide from a marsh soil, *J. Atmos. Chem.*, **17**, 249–275, 1993.
- Rudolph, J., and R. Conrad, Flux between soil and atmosphere, vertical concentration profiles in soil, and turnover of nitric oxide, II, Experiments with naturally layered soil cores, *J. Atmos. Chem.*, **23**, 275–300, 1996.
- Schmidt, I., and E. Bock, Anaerobic ammonia oxidation with nitrogen dioxide by *Nitrosomonas eutropha*, *Arch. Microbiol.*, **167**, 106–111, 1997.
- Schwartz, S. E., Factors governing dry deposition of gases to surface water, in *Precipitation Scavenging and Atmosphere–Surface Exchange*, edited by S. E. Schwartz and W. G. N. Slinn, 2, 789–801, Taylor and Francis, Philadelphia, Pa., 1992.
- Tomasella, J., and M. G. Hodnett, Estimating soil water retention characteristics from limited data in Brazilian Amazonia, *Soil Sci.*, **163**, 190–202, 1998.
- van Cleemput, O., and L. Baert, Theoretical considerations on nitrite self-decomposition reaction in soil, *Soil Sci. Soc. Am. J.*, **40**, 322–324, 1976.
- van Cleemput, O., and L. Baert, Nitrite: a key compound in N loss processes under acid conditions?, *Plant Soil*, **76**, 233–241, 1984.
- van Dijk, S. M., A. Gut, G. A. Kirkman, B. M. Gomes, F. X. Meixner, and M. O. Andreae, Biogenic NO emissions from forest and pasture soils: Relating laboratory studies to field measurements, *J. Geophys. Res.*, **107**(XX), 10.1029/2001JD000358, in press, 2002.
- Verchot, L. V., E. A. Davidson, J. H. Cattanio, I. L. Ackerman, H. E. Erickson, and M. Keller, Land use change and biogeochemical controls of nitrogen oxide emissions from soils in eastern Amazonia, *Glob. Biogeochem. Cycles*, **13**, 31–46, 1999.
- Villá-Guerrau de Arellano, J., and P. G. Duynkerke, Influence of chemistry on the flux–gradient relationships for the NO–NO<sub>3</sub>–NO<sub>2</sub> system, *Boundary Layer Meteorol.*, **61**, 375–387, 1992.
- Wesely, M. L., Parameterization of surface resistances to gaseous dry deposition in regional-scale numerical models, *Atmos. Environ.*, **23**, 1293–1304, 1989.
- Wesely, M. L., and B. B. Hicks, Some factors that affect the deposition rates of sulfur dioxide and similar gases on vegetation, *J. Air Pollut. Control Assoc.*, **27**, 1110–1116, 1977.
- Wesely, M. L., and B. B. Hicks, A review of the current status of knowledge on dry deposition, *Atmos. Environ.*, **34**, 2261–2282, 2000.
- Winer, A. M., J. W. Peters, J. P. Smith, and J. N. Pitts, Jr., Response of commercial chemiluminescent NO–NO<sub>2</sub> analyzers to other nitrogen-containing compounds, *Environ. Sci. Technol.*, 1118–1121, 1974.
- Zart, D., and E. Bock, High rate of anaerobic nitrification and denitrification by *Nitrosomonas eutropha* grown in a fermenter with complete biomass retention in the presence of gaseous NO<sub>2</sub> and NO, *Arch. Microbiol.*, **169**, 282–286, 1998.

---

C. Ammann, M. O. Andreae, A. Gut, G. A. Kirkman, and F. X. Meixner, Biogeochemistry Department, Max Planck Institute for Chemistry, P.O. Box 3060, D-55020, Mainz, Germany. (grant@mpch-mainz.mpg.de; meixner@mpch-mainz.mpg.de)

L. V. Gatti and A. M. Cordova, Divisão de Química Ambiental, Instituto de Pesquisas Energéticas e Nucleares (IPEN), São Paulo, Brazil.

M. A. L. Moura, Departamento de Meteorologia, Centro de Ciencia Exatas e Naturais, Universidade Federal de Alagoas, Maceió, Alagoas, Brazil.